AD-A065 741 UNITED TECHNOLOGIES CORP SUNNYVALE CALIF CHEMICAL SY--ETC F/G 21/9.2
ROTATING VALVE FOR VELOCITY COUPLED COMBUSTION RESPONSE MEASURE--ETC(U)
FEB 79 R S BROWN, R C WAUGH F49620-77-C-0048

UNCLASSIFIED CSD-2624-ISR-2 AFOSR-TR-79-0247 NL

1 OF 1
AD
AD 65741

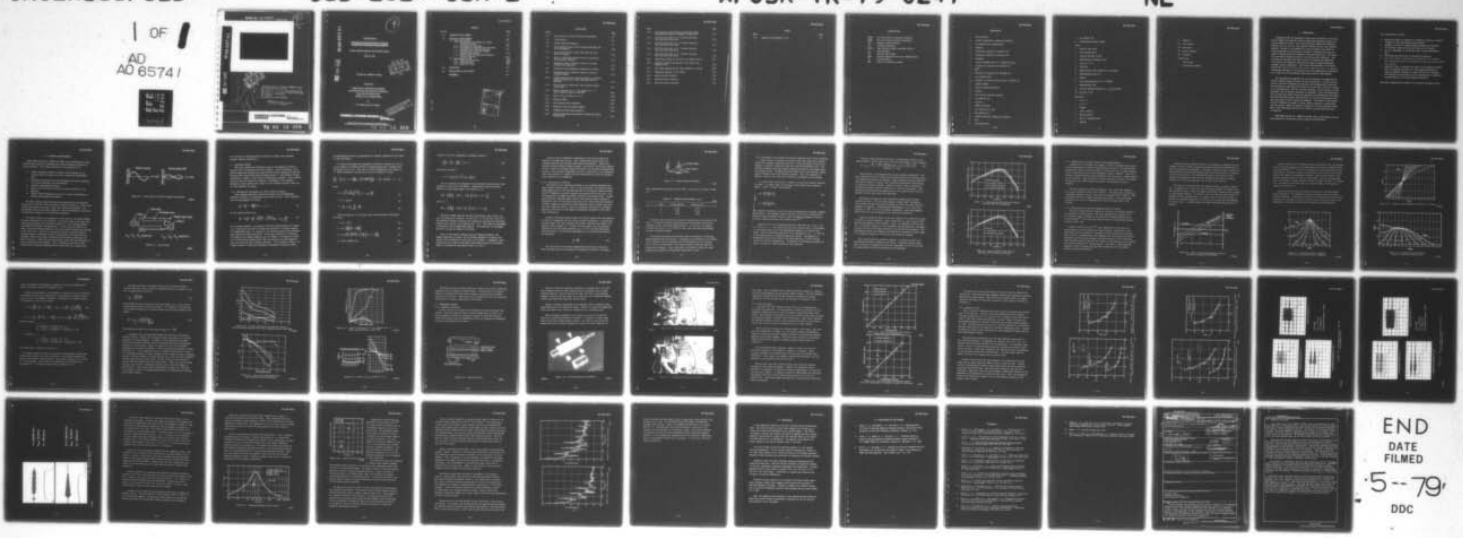

END
DATE FILMED
5-79
DDC

AIR FORCE OFFICE OF SCIENTIFIC RESEARCH (AFSC)
NOTICE OF TRANSMITTAL TO DDC
This technical report has been reviewed and is approved for public release IAW AFR 190-12 (7b).
Distribution is unlimited.
A. D. BLOSE
Technical Information Officer

Approved for public release;
distribution unlimited.

CHEMICAL SYSTEMS DIVISION
UNITED TECHNOLOGIES

(4)

CSD 2624-ISR-2

ROTATING VALVE FOR VELOCITY COUPLED COMBUSTION RESPONSE MEASUREMENTS

Annual Technical Report/Interim Scientific Report

February 1979

Contract No. F49620-77-C-0048

Prepared for

DIRECTOR OF AEROSPACE SCIENCES
AIR FORCE OFFICE OF SCIENTIFIC RESEARCH
BOLLING AIR FORCE BASE
DISTRICT OF COLUMBIA 20332

by

R. S. Brown and R. C. Waugh

CHEMICAL SYSTEMS DIVISION
UNITED TECHNOLOGIES

CONTENTS

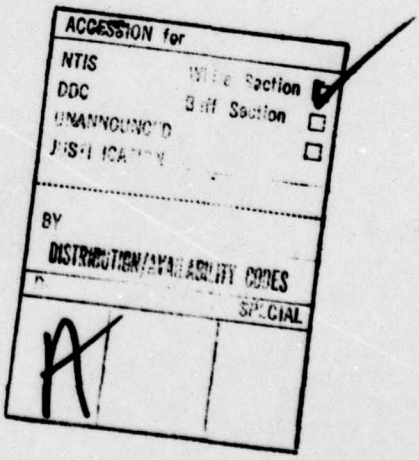

ILLUSTRATIONS

TABLES

ABBREVIATIONS

AFOSR	Air Force Office of Scientific Research
AFRPL	Air Force Rocket Propulsion Laboratory
CSD	Chemical Systems Division
FM	frequency modulation
HIPPO	high internal pressure producing orifice
ID	inner diameter
IUS	inertial upper stage
NASA	National Aeronautics and Space Administration
OD	outside diameter
OSR	Office of Scientific Research

NOMENCLATURE

a	sonic velocity
A	acoustic admittance, combustion parameter
C	see equation (8), concentration
d	diameter
D	integration constant in equation (12)
E	integration constant in equation (12)
f	frequency
F	particle damping term ($F' = i\lambda C_m M'/(1+i\lambda\tau_d)$)
G	parameter in equation (19) through (21)
i	$\sqrt{-1}$
I	parameter in equation (19) through (21)
k	see equation (10)
K_1	parameter in equation (21) defined in figure 2-8
L	chamber length
m	velocity coupling parameter
M	Mach No.
n	burning ratio pressure exponent
N	see equation (9)
p	pressure
q	chamber perimeter
Q	see equation (4), $f/\Delta f$
r	see equation (7)
R	response function, combustion parameter
S	area
T	see equation (5)

Y	see equation (6)
Z	dimensionless chamber length

Greek

γ	specific heat ratio
Γ	time constant ratio
ϵ	acoustic pressure ($p'/\gamma\bar{p}$)
λ	dimensionless frequency $2\pi fL/a$
λ	$\lambda_1(\lambda_1-1) = i\lambda\Gamma$
μ	viscosity
ω	dimensionless flame temperature oscillation
ψ	dimensionless area $S'/\bar{S}$
ρ	density
σ'	flow turning parameter ($\sigma' = M' d\bar{M}/dZ$)
τ	dimensionless time
τ_d	particle damping parameter ($\tau_d = \bar{a}d_p^2\rho_p/(18\mu L)$)
$\bar{\chi}_1$	$\bar{S}_{vo}/(\bar{S}_{vo} + \bar{S}_{v1})$

Subscripts

o	at Z = 0
1	at Z = 1
c	chamber
v	valve, velocity
b	burning surface
m	mass of condensed phase
d	damping

p particle

FT flow turning

MS mean shift

DF double frequency

TH threshold

Superscripts

- time average

′ oscillating component

1.0 INTRODUCTION

Coupling between the combustion process and the acoustics of the combustion chamber are important factors determining combustion stability of a solid propellant rocket. This coupling results because the combustion process reacts to both the local acoustic pressure and the local acoustic velocity. Because of the complexity of both processes, they cannot be totally characterized analytically; therefore, laboratory test data are needed in making analytical combustion stability predictions. One attractive test method conceived by CSD is the rotating valve apparatus. CSD conducted two programs under AFRPL contract to develop and demonstrate the rotating valve method of measuring the pressure coupled combustion response of solid propellants. The results show agreement with T-burner measurements when the T-burner vent term is taken to be zero. In addition, reproducible operation of the apparatus has been demonstrated at pressures up to 1,500 psi with propellants containing as much as 18% aluminum.

The rotating valve apparatus also has the potential for measuring the velocity coupled response function of solid propellants. Velocity oscillations of controlled frequency and amplitude can be generated by simultaneously operating a rotating valve at each end of the motor, 180° out of phase. In this configuration, velocity coupling dominates, and the effects of other processes, such as pressure coupling, are minimized. With this modification, the rotating valve method offers the potential for experimentally and quantitatively investigating many characteristics of velocity coupling which have been postulated by purely analytical arguments. The nature of these characteristics determine the manner in which velocity coupling is incorporated into the overall combustion stability analysis of a solid propellant rocket motor; thus experimental evaluation of velocity coupling characteristics is essential.

Under AFOSR contract No. F49620-77-C-0048, CSD is investigating the two-valve approach for measuring velocity coupling characteristics.

This investigation includes:

A. Analytical studies to analyze the transient ballistics to provide a method for data interpretation and analysis
B. Parametric studies to evaluate momentum effects and determine the frequency range for which valid data can be obtained
C. An error assessment of the methods used to reduce experimental data
D. The design and fabrication of experimental apparatus
E. Cold flow studies to evaluate the performance of the apparatus and to develop methods for calibrating the apparatus for data reduction purposes
F. Combustion tests to evaluate the limits of the apparatus performance, to determine the ability to distinguish differences in velocity response functions, to study the effects of internal flow patterns on the derived velocity response, and to establish the applicability of the data analysis procedures.

This report summarizes the results of the studies concluded to date.

2.0 TECHNICAL ACCOMPLISHMENTS

Under AFOSR contract No. F49620-77-C-0048, CSD is developing the dual rotating valve approach for measuring the velocity response properties of solid propellants. The primary objectives of this program are to:

A. Conduct analytical studies to predict the performance of the apparatus and to provide a basis for interpreting experimental data
B. Evaluate potential errors in the experiment and thereby determine the accuracy required in the measurements
C. Construct experimental apparatus
D. Conduct cold flow tests to verify the proper operation of the apparatus
E. Conduct limited combustion tests over a range of frequencies to evaluate the apparatus performance

The basic velocity coupled rotating valve apparatus has two identical valves, one at each end of the test motor as shown in figure 2-1. One or more conventional nozzles are used to control the steady-state pressure. The instantaneous area of each valve (figure 2-1) may be represented by the sum of a steady-state component and an oscillating component.

The central feature of the apparatus is the control of the phase between the area oscillations of the two valves. If the two valves are in phase, the oscillating components add, as shown in figure 2-2. The resulting behavior is dominated by pressure coupling effects. If the valves are 180^{o} out of phase, the area oscillation produced by one valve exactly cancels that produced by the other valve. There is no net area oscillation to provide pressure coupling; however, significant velocity oscillations in the test motor are produced, because the venting of combustion gas alternates between the two ends of the motor. These velocity oscillations couple with the combustion to produce burning rate oscillations. With a constant net vent area, these burning rate oscillations operating the two valves 180^{o} out of phase offer

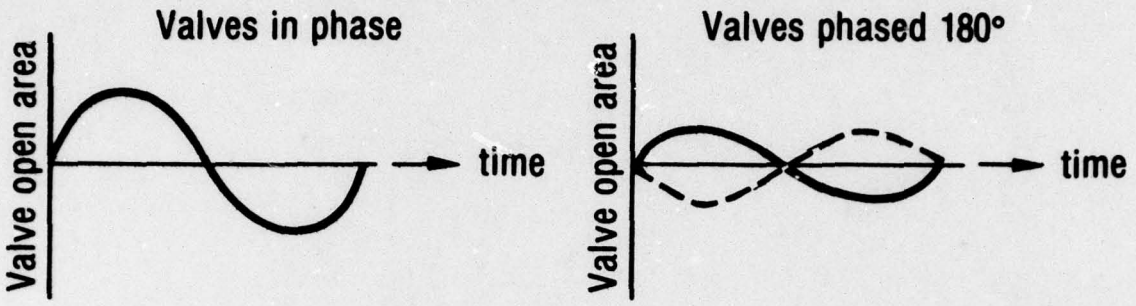

Figure 2-1. Valve Layout for Velocity Response Measurement

08882R

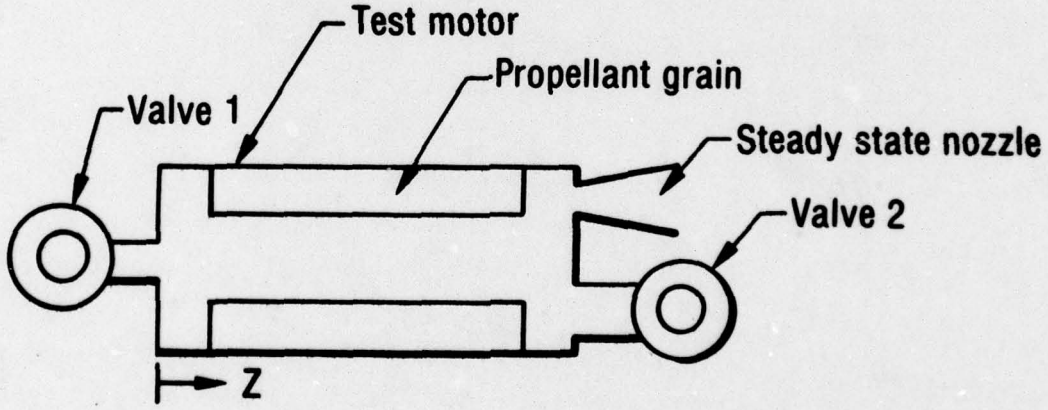

$$S_{v_1} = \bar{S}_{v_1} + \hat{S}_{v_1} \exp(i2\pi ft) \qquad S_{v_2} = \bar{S}_{v_2} + \hat{S}_{v_2} \exp(i2\pi ft)$$

Figure 2-2. Valve Driving

08883R

the potential for studying velocity coupling in a manner that minimizes pressure coupled contributions.

2.1 ANALYTICAL STUDIES

Analytical studies were conducted as part of the program to provide a basis for data interpretation and error analysis. Initial evaluation of the method assumed that momentum and energy effects could be neglected so that the transient mass balance described the system behavior.[1] The validity of these assumptions is suspect in the velocity coupled mode; therefore, a more detailed and less restricted analysis is required. Development of the expanded mathematical model requires the solution of the transient ballistic equations for mass, momentum and energy.

2.1.1 Mathematical Development for Linear Velocity Coupling

These expanded analytical studies are based on the one-dimensional equations of motion, in conjunction with the ideal gas law. After linearization and rearrangement one obtains

$$\frac{\partial \varepsilon'}{\partial Z} + \frac{\partial M'}{\partial \tau} + \frac{\partial (\bar{M} \cdot M')}{\partial Z} + \sigma' - F' = 0 \qquad (1)$$

for the momentum equation and

$$\frac{\partial \varepsilon'}{\partial \tau} + \bar{M} \frac{\partial \varepsilon'}{\partial Z} + \frac{\partial M'}{\partial Z} = \left(\frac{A_b q L}{S}\right) \varepsilon' + \left(\frac{\bar{M}_b q L}{S}\right) \left(R_b + \omega_f\right)_v \frac{\bar{M} \cdot M'}{|\bar{M}|} \qquad (2)$$

for the energy equation. It should be noted that these equations are identical to those used by Culick[2] to estimate the stability of acoustic chambers for longitudinal waves. At this point, the solutions proceed along different paths because the objectives differ. Culick was interested in calculating the change in the complex eigenvalue for the chamber to determine the stability of self-excited acoustic waves; thus, his solution uses approximations which are valid only near resonant conditions. In this project, however, the primary interest is the burner response to nonresonant frequencies; hence,

the approximations which are appropriate for resonant conditions are not valid in this development.

To obtain the solution for nonresonant conditions, equations (2) and (3) can be combined to eliminate dM'/dZ by assuming separation of variables and replacing $\partial()/\partial\tau$ by $i\lambda()$. The result is then differentiated with respect to Z. Terms containing M' and dM'/dZ can then be eliminated to yield

$$\frac{d^2\varepsilon'}{dZ^2} - \left[\bar{M}\left(T + Q + \frac{2d\bar{M}}{dZ}\right) + Y\left(\frac{Q + d\bar{M}/dZ}{Q}\right)\right]\frac{d\varepsilon'}{dZ} - T\left(Q + d\bar{M}/dZ\right)\varepsilon' = 0 \quad (3)$$

where

$$Q \equiv i\lambda\left(\frac{1 + C_m + i\lambda\tau_d}{1 + i\lambda\tau_d}\right) + (1 - R_{FT})\frac{d\bar{M}}{dZ} \quad (4)$$

$$T \equiv i\lambda - A_b qL/S_c \quad (5)$$

$$Y \equiv \left(R_b + \omega_f\right)_v \frac{\bar{M}}{|\bar{M}|} \cdot \frac{d\bar{M}}{dZ} \quad (6)$$

Note that equation (3) is second order and has variable coefficients. By letting

$$r \equiv (CZ - N)^2/C \quad (7)$$

$$C \equiv 0.5\left(\frac{d\bar{M}}{dZ}\right)\left(Q + T + \frac{2d\bar{M}}{dZ}\right) \quad (8)$$

$$N \equiv -0.5Y\left(\frac{Q + d\bar{M}/dZ}{Q}\right) + \frac{\chi_1}{2}\frac{d\bar{M}}{dZ}\left(Q + T + 2\frac{d\bar{M}}{dZ}\right) \quad (9)$$

$$k \equiv T\left(Q + d\bar{M}/dZ\right)/(4C) \quad (10)$$

equation (3) can be transformed to a Kummers equation.[3]

$$r\frac{d^2\epsilon'}{dr^2} + \left(\frac{1}{2} - r\right)\frac{d\epsilon'}{dr} - k\epsilon' = 0 \tag{11}$$

The solution becomes [4]

$$\epsilon' = D\,K\left(k,\frac{1}{2},r\right) + Er^{\frac{1}{2}}\,K\left\{k+\frac{1}{2},\frac{3}{2},r\right\} \tag{12}$$

The two constants of integration can be evaluated from the nozzle flow equations at each end of the chamber. Assuming the nozzles and valves behave in a quasi-steady manner, one finds at Z = 0

$$QM'_o = \left(\frac{-d\epsilon'}{dZ}\right)_o + \bar{M}_o T\epsilon'_o = Q\bar{M}_o\left[0.5\epsilon'_o(\gamma - 1) + \psi_o\right] \tag{13}$$

and at Z = 1

$$QM'_1 = \left(\frac{-d\epsilon}{dZ}\right)_1 + \bar{M}_1 T\epsilon'_1 = Q\bar{M}_1\left[0.5\epsilon'_1(\gamma - 1) + \psi_1\right] \tag{14}$$

Because Y changes sign when the mean flow Mach No. goes to zero, two sets of constants are required: one set for $0 < Z < \bar{X}_1$ and one for $\bar{X}_1 < Z < 1$. The additional boundary conditions are obtained by requiring the oscillatory pressure and velocity to be continuous for $Z = \bar{X}_1$. This model was programmed in Fortran for the Burroughs 6700 computer. The definition for the Kummer Function[4] was used to evaluate this series.

Thus, if the acoustic response, particle damping parameters, and chamber dimensions are known, the oscillating components of pressure and velocity can be predicted for any point in the chamber. Furthermore, these predictions can be made for any phase relationship between the two valves, simply by selecting the appropriate value of ψ_o and ψ_1.

There are several significant advantages to this solution beyond the simplified analysis used earlier. First, momentum and energy effects are included along with the transient mass balance contributions. Second, the analysis includes pressure coupled response, flow turning, and particle damping effects. Third, the analysis permits the study of the two-valve configurations as well as the one-valve configuration and is not restricted to low frequencies. Thus, this analysis is a general solution which should be valid for one-dimensional burners at all frequencies.

2.1.2 Verification of Solution

The solution of the equations described in the preceding paragraphs has been checked in several ways. First, at low frequencies, the equations should reduce analytically to the equations derived for the pressure coupled rotating valve,[5,6] assuming no velocity response and driving from only one valve. For low frequencies, the Kummer functions in equation (12) approach unity. Following through the resulting algebra leads to the identical result reported in references 5 and 6 for the case of one valve and for both valves when operated in phase. Numerical calculations using appropriate inputs to model this case also yield identical results. This is an important point since it provides a numerical verification of the computer programming in addition to the analytical verification.

Secondly, this model should predict the correct behavior when the combustor is driven at frequencies near the natural acoustic frequencies. In particular, one would expect that near resonance the pressure amplitude would exhibit the behavior shown in figure 2-3. Further, one would expect that the frequency difference at the half-power amplitudes (i.e., 0.707 x the peak amplitudes) would be related to the overall system damping of the self-excited system by the expression

$$\frac{\alpha}{f} = \frac{\pi \Delta f}{f} \qquad (15)$$

The left side can be evaluated independently from Culick's solutions while the right side can be evaluated from numerical solutions of the model.

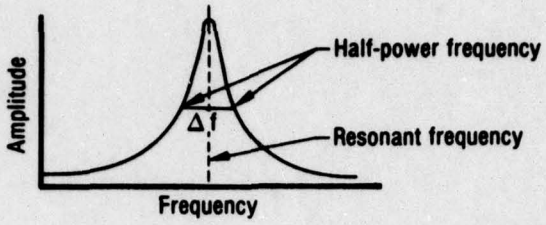

Figure 2-3. Dynamic Amplitude Response

12933

This comparison has been made in three cases. The results are shown in table 2-1.

TABLE 2-1. COMPUTED SYSTEM DAMPING ($-\alpha/f$)

T4126

Case	Culick Analysis	Equation (12)
1	0.112	0.117
2	0.155	0.156
3	0.102	0.108

The first case contained only pressure coupling effects and used only one valve. The second and third cases incorporated both pressure and velocity coupling, as well as particle damping effects. In case two, the response functions were low (i.e., 0.2) while in case three, they were approximately an order of magnitude higher.

The excellent agreement found between these two methods for predicting damping substantiates the analysis. Furthermore this demonstrates the analysis is not limited to the low frequency bulk flow conditions of the rotating valve, but is also applicable to the higher frequency conditions near the acoustic mode frequency. Thus, this model could provide a basis for interpreting data obtained in the modulated throat motor as well.

2.1.3 Development of Data Reduction Procedure Assuming Linear Velocity Coupling

A large variety of numerical calculations have been conducted to examine methods for obtaining approximate solutions. These approximate solutions are required to provide a convenient method for reducing experimental data. The analysis presented previously predicts pressure and velocity performance given the response values. The data analysis procedure must do the opposite, namely produce response values from measured pressures. Since the responses are implicit, equation (12) cannot be conveniently rearranged for this purpose.

To conduct these calculations, a method for predicting response functions is needed. A rational basis is provided by using thermal wave combustion models. Brown,[7] Culick,[8] and Lengellé[9].

$$R_p = \frac{n(1 + A - R)}{\lambda_1 + A/\lambda_1 - R} \tag{16}$$

and

$$R_v = \frac{m(1 + A - R)}{\lambda_1 + A/\lambda_1 - R} \tag{17}$$

The combustion parameters A and R can then be determined from pressure response measurements. The parameter m must be selected arbitrarily, although unity appears to give reasonable values in terms of limited experimental values of velocity response functions from T-burner tests.[10,11]

Using values for the aluminized propellant, ANB 3066, ($A = 15$, $R = 4.97$, $n = 0.27$, $m = 1$, $\Gamma = 31.5$) and the valves out of phase by 180°, a large number of calculations were run for the experimental geometry to be used in this study. These calculations showed that at low frequencies (i.e., $\lambda = 0.75$) the oscillating velocity is essentially spatially uniform. The magnitude is determined strictly by the size of the oscillating area of the two valves relative to the time-averaged area. In addition, the oscillating pressure is shown to be nearly a linear function of axial position.

Using the linear pressure observation, an approximate solution of the energy equation, which is explicit in the velocity response, can be developed.

$$(R + \omega_f)_v = \frac{T\varepsilon'_o + \left(2T + d\bar{M}/dZ\right)\chi_1\left(\varepsilon'_1 - \varepsilon'_o\right) + \left(M'_1 - M'_o\right)}{(d\bar{M}/dZ)M'_1\,(1 - 2\chi_1)} \qquad (18)$$

The accuracy of this approximation has been examined numerically. The exact solution was used to predict oscillating pressures and velocities using the combustion parameters for ANB 3066. These pressures and velocities were then used as inputs to equation (18), simulating experimental observations, to derive the velocity response. Figures 2-4 and 2-5 show a comparison of the derived and exact velocity response for a variety of conditions. This comparison is made using the imaginary part of the response since this is a parameter used in motor stability predictions.

The results in figure 2-4 were obtained by assuming the propellant contained no metal. With the valves phased by exactly 180°, the maximum error between the input and derived response is ±10% at the point where the response is a maximum. Including phase misalignments of 3.5°, this error increases to ±20%. As will be discussed subsequently, phase misalignments greater than ±3.5 may be expected in the experimental apparatus.

Figure 2-5 shows the effect of particle damping on the comparison between the exact and derived response. These calculations were made using the maximum particle damping at each frequency. Again, the agreement is better than 10%. It therefore appears that the approximate analysis provides a reasonably accurate solution at the lower frequencies for the conditions examined. This approximate solution also suggests a good method for estimating initial inputs if the complete analysis is required for data reduction purposes.

More studies should be conducted, however, to examine the effect of a larger phase difference between the two valves. Additional studies should also be conducted to examine the effects of experimental errors in the pressure measurements and the oscillating velocity magnitudes.

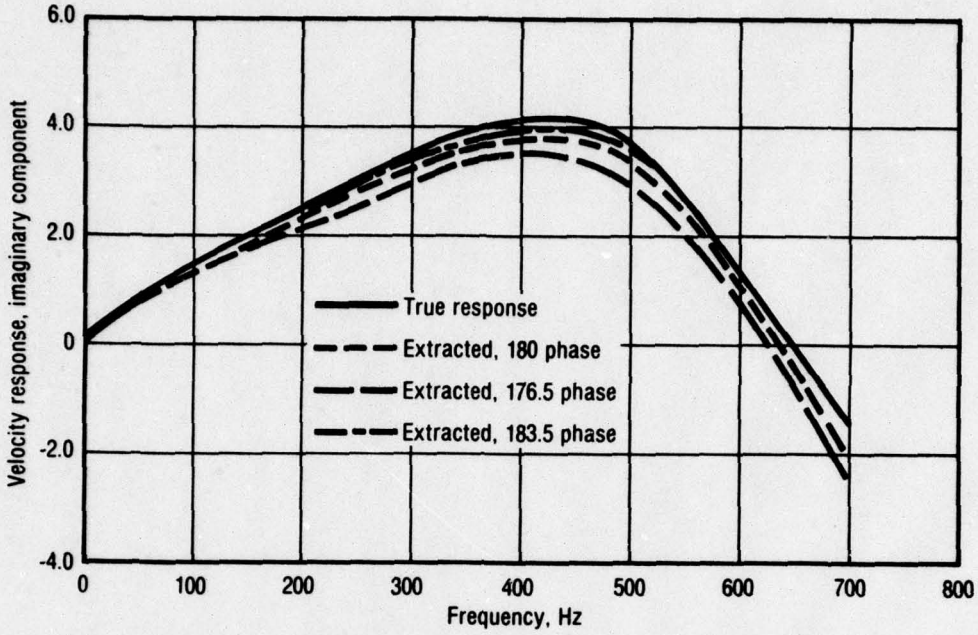

Figure 2-4. Error Analysis Study Velocity Response ANB 3066 (No Particle-Damping)

12934

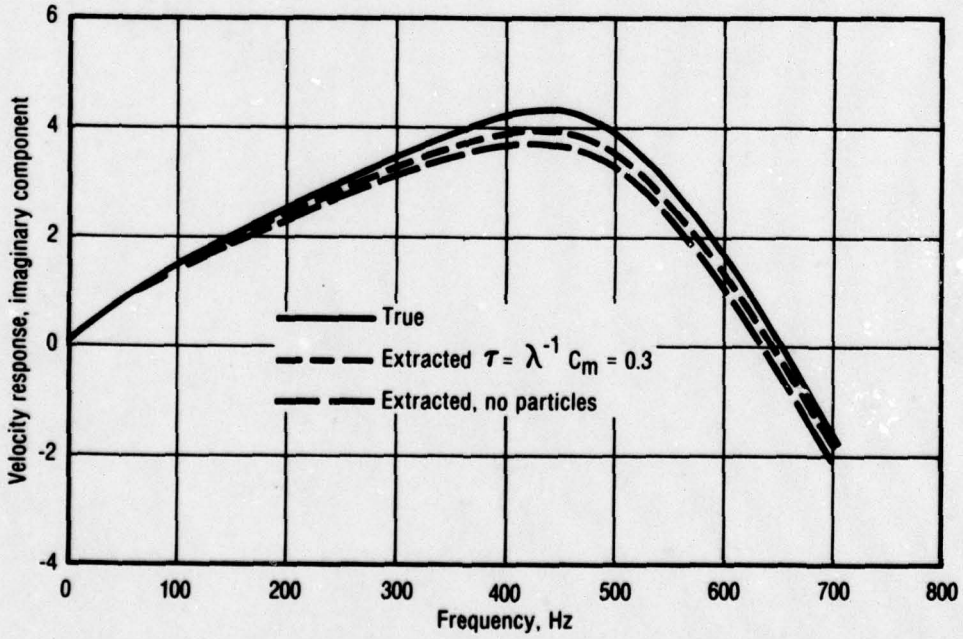

Figure 2-5. Error Analysis Study Velocity ANB 3066 (Particle Effects Included)

12935

2.1.4 Implications in Pressure Coupled Response Measurements

Examination of this model also suggests a method for significantly improving the measurement of pressure coupled response functions. The single-valve configuration, which is currently used for this purpose, has an upper frequency limit of approximately 25% of the fundamental acoustic frequency. Above this frequency, momentum effects become significant and the burner no longer operates in the bulk mode. Using two valves in phase, numerical solutions of the model indicate that this limit becomes about 40% of the fundamental acoustic frequency.

This has significant practical importance. The current CSD apparatus has an upper frequency limit of 700 to 800 Hz. Using two valves in phase and a shortened combustion section, this limit would become 1400 to 1500 hz. Thus, this method will have an upper frequency limit similar to the conventional T-burner but it can go to frequencies well below the lower limit of the T-burner.

2.1.5 Modifications for Amplitude Dependent Velocity Coupling

The form in which velocity coupling is included in the analysis needs to be considered in further detail. The form incorporated in equation (2) is the classical linear form which is included in the Standard Stability Prediction Program.[12] This form also forms the basis for interpreting velocity coupled T-burner data.

However, Culick[8] and Price[13,14] have suggested that there may be an analog between velocity coupling and erosive burning. Specifically, this means there may be a minimum, or threshold, velocity which must be exceeded before there is coupling between the combustion and the velocity oscillations. Both Culick and Price have discussed the characteristics of this conceptual model in detail and have shown how the effects of flow reversal and the threshold velocity influence the coupling process. This model, called amplitude dependent velocity coupling, has also been incorporated in the Standard Stability Prediction Program.[12]

Studies have been conducted as part of this program to determine how the threshold and flow reversal effects would modify the predicted ballistics of the dual rotating valve experiment. The basic concepts are show in figure 2-6, which shows the total velocity profile (mean plus oscillations) as a function of axial motor position. The threshold velocity is also shown for both positive and negative velocities on the assumption that velocity coupling depends on the local gas magnitude, but not the local direction.

The motor can be divided into five separate regions, as shown in figure 2-6. In regions 1 and 5, the local velocity always exceeds the threshold and the coupling is linear. Hence the analysis described previously can be coupled to these regions directly. In region 3, the local velocity never exceeds the threshold and no coupling occurs. In regions 2 and 4, the local velocity exceeds the threshold during part of the cycle and is less than the threshold part of the cycle. In these regions, the model described previously must be modified.

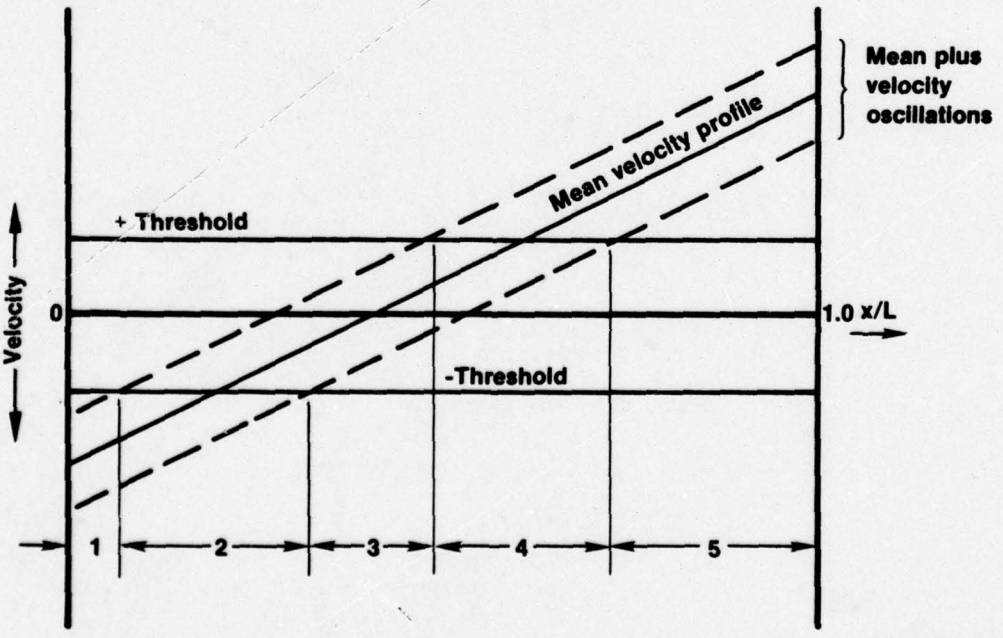

Figure 2-6. Effect of Amplitude-Dependent Velocity Coupling on Rotating Valve Response

V-10464

The basic approach to incorporating these modifications into the analysis follows the methods used in the Standard Stability Prediction Program[12] and by Price and Dehority.[13,14] The wave is decomposed into the appropriate Fourier coefficients. Parametric studies were then made to show how the time average burning rate shift, the fundamental component, and the second harmonic vary with the threshold velocity, the mean flow velocity, and the velocity amplitude. The results of these parametric studies are shown in figure 2-7 through 2-9. It should be noted that figure 2-8 contains identical information to figure 8 of reference 14.

The most striking result from these calculations is the approximately linear variation of the fundamental component with mean flow for constant velocity amplitude. Calculations with the model described previously show the amplitude of oscillating velocity is nearly constant along the burner at low frequencies. Since the mean flow varies linearly with axial position,

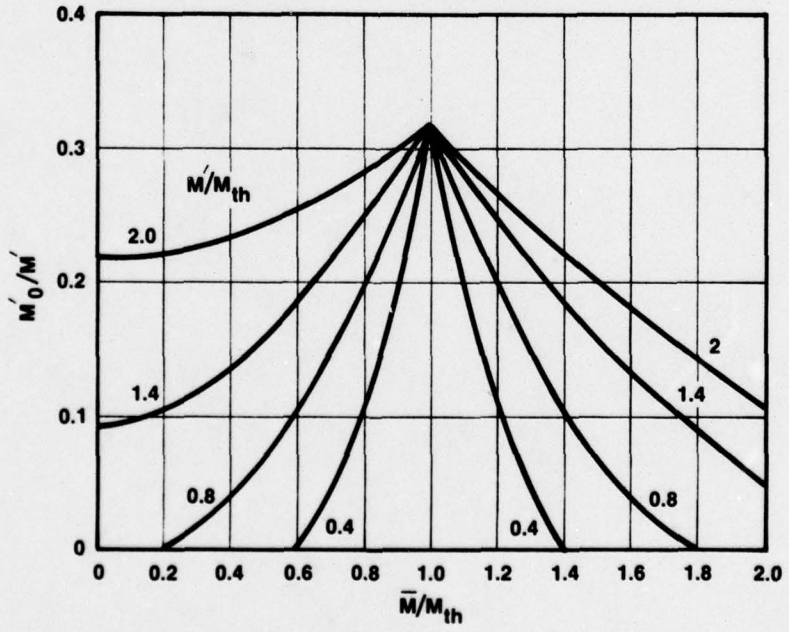

Figure 2-7. Parametric Study of Harmonic Content in Driving (Steady State Component)

V-10465

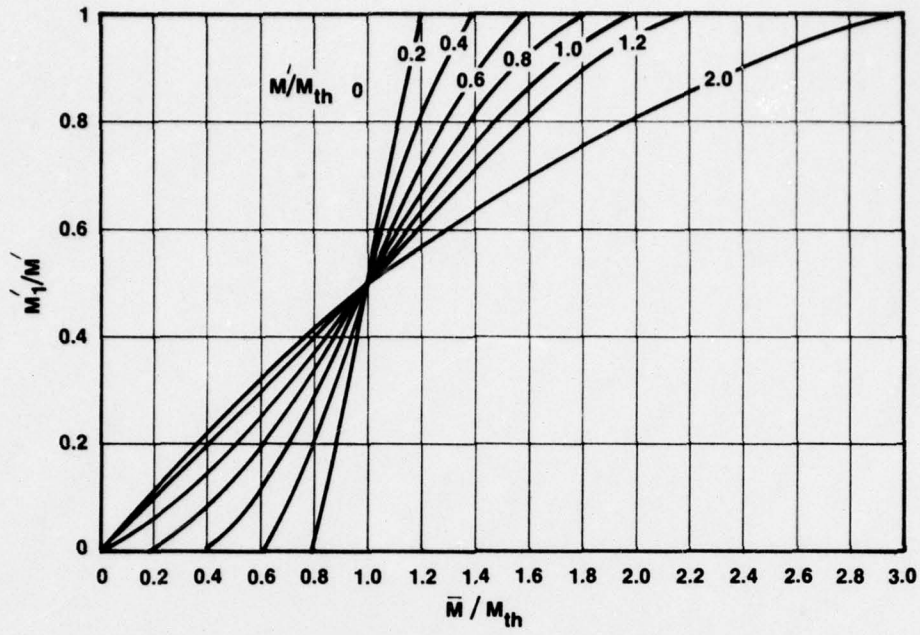

Figure 2-8. Parametric Study Fundamental Component of Driving

V-10466

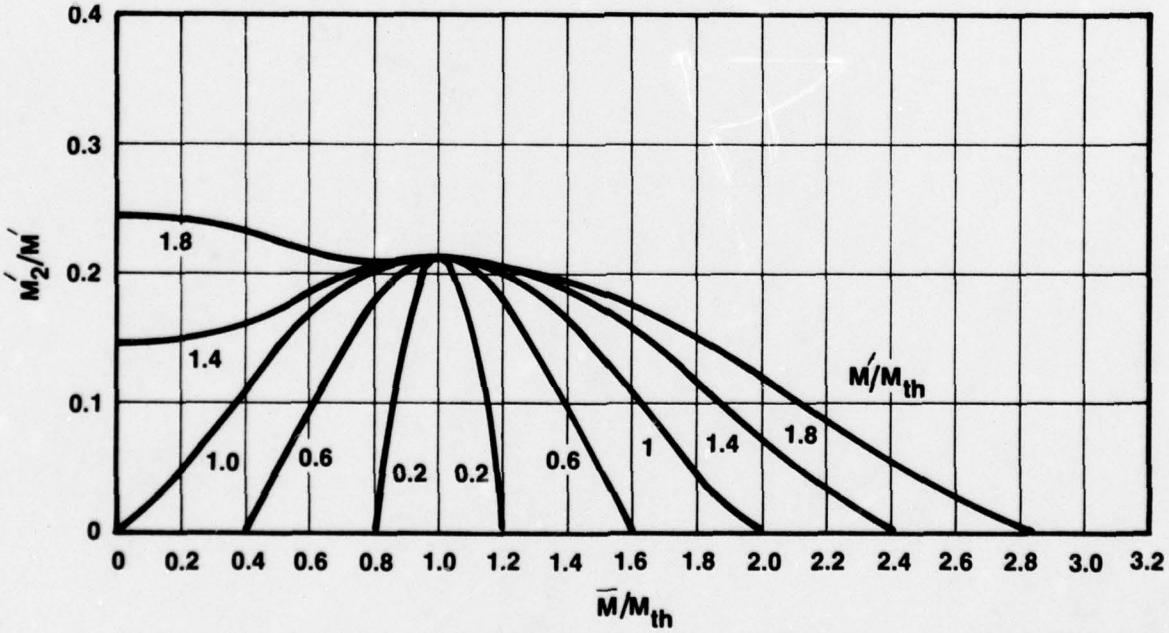

Figure 2-9. Parametric Study of Harmonic Content in Driving (Second Harmonic)

V-10467

figure 2-8 suggests the fundamental component of velocity coupling varies linearly with axial position in regions 2 and 4.

Using this approximation, the parameters in equation (3) can be redefined and thereby solutions can be obtained for the pressure and velocity oscillations in terms of the Kummer's Functions. Specifically, in regions 2 and 4, the parameters C and N are as follows:

$$C = 1/2 \left\{ \frac{dM}{dZ} \left[T + Q + 2\frac{dM}{dZ} \right] - I(R_b + \omega_f)_v \frac{dM}{dZ} G_c \left[\frac{Q + \frac{dM}{dZ}}{Q} \right] \right\} \quad (19)$$

$$N = -1/2 \left\{ -\psi_o \frac{dM}{dZ} \left[T + Q + 2\frac{dM}{dZ} \right] + I(R_b + \omega_f)_v \frac{dM}{dZ} G_N \left[\frac{Q + \frac{dM}{dZ}}{Q} \right] \right\} \quad (20)$$

Where in region 2:

$$I = -1$$
$$G_c = \left[K_1(Z_1) - K_1(Z_2) \right] / (Z_2 - Z_1)$$
$$G_N = K_1(Z_2) + (Z_2) \left[K_1(Z_1) - K_1(Z_2) \right] / (Z_2 - Z_1).$$

In region 4:

$$I = +1$$
$$G_c = \left[K_1(Z_4) - K_1(Z_3) \right] / (Z_4 - Z_3)$$
$$G_N = K_1(Z_3) + (Z_3) \left[K_1(Z_4) - K_1(Z_3) \right] / (Z_4 - Z_3)$$

(The function K_1 is defined on figure 2-8.)

With these changes, the motor is divided into five regions, rather than the two regions used in the truly linear case. The acoustic pressure and velocity are matched at each interface. The boundary condition at Z = 0 and Z = 1 are unchanged. Thus, there are 10 equations and 10 unknown to be determined (i.e., the unknown coefficients in equation (12).)

Estimates were made of the mean burning rate shift and the double-frequency amplitude using the Fourier decompositions shown in figure 2-7 and 2-9. The mean shift is given by:

$$\varepsilon_{MS} = \frac{R_{vo}\langle M'_{MS}\rangle}{\gamma(1 - n)} \tag{22}$$

where $\langle\ \rangle$ indicates the average over the burner length. R_{vo} is the velocity coupled response function at zero frequency. The estimate of the amplitude at the double frequency was evaluated assuming the bulk mode response of the chamber

$$\varepsilon_{DF} = \frac{-R_{v2}\langle M'_{DF}\rangle}{\gamma R_{p_2} + \frac{1 - 3\gamma}{2} - \frac{2i\lambda}{M_b qL/S}} \tag{23}$$

The response functions are at the double frequency $2\lambda = \frac{4\pi fL}{a}$.

A parametric study was performed assuming the propellant followed the thermal lag model. Figures 2-10 through 2-12 show the results for a typical propellant and burner geometry. In figure 2-10 the amplitude of pressure oscillation follows the general trend of decreasing amplitude with frequency expected for the bulk mode. Figure 2-11 shows the ratio of the pressure amplitudes at each end of the burner. The corresponding phase angles are shown in figure 2-12. In the amplitude ratio vs. frequency curve there is a trend of the minimum shifting to a lower frequency as the threshold velocity increases. The plot of phase in figure 2-12 shows that the $M_{th} = 0.03$ curve has a different character from the other three curves. For $M_{th} = 0.03$, all the velocities are less than the threshold and no coupling occurs. There is a drastic change from $M_{th} = 0.02$ to 0.03. Additional cases were run to see this change in greater detail. These cases, which are presented in figure 2-13, show that as the amount of velocity coupling approaches zero, the character of the phase curve changes rapidly.

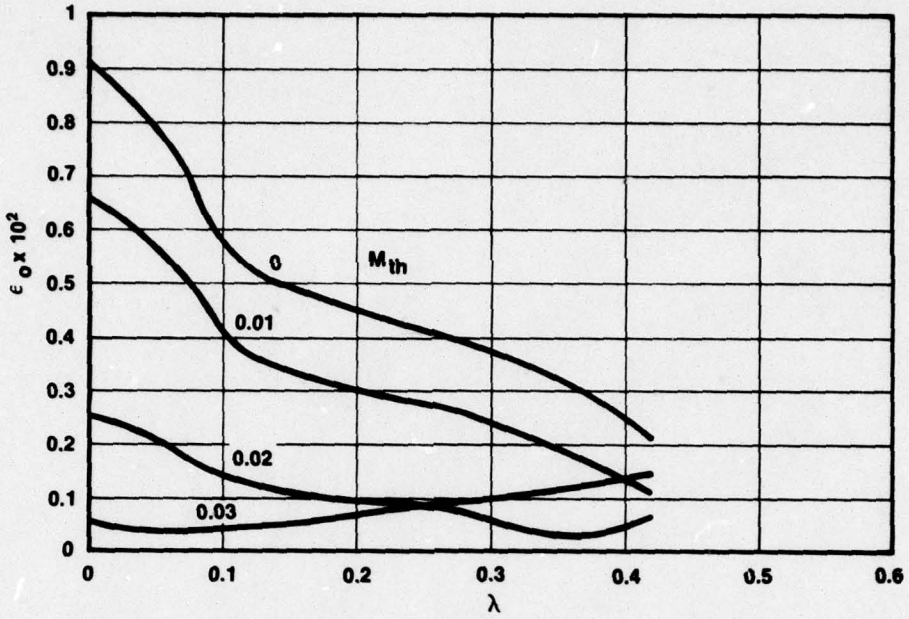

Figure 2-10. Pressure Amplitude from Analytical Model of Velocity-Coupled Rotating Valve (Input Responses Based on ANB 3066)

V-10468

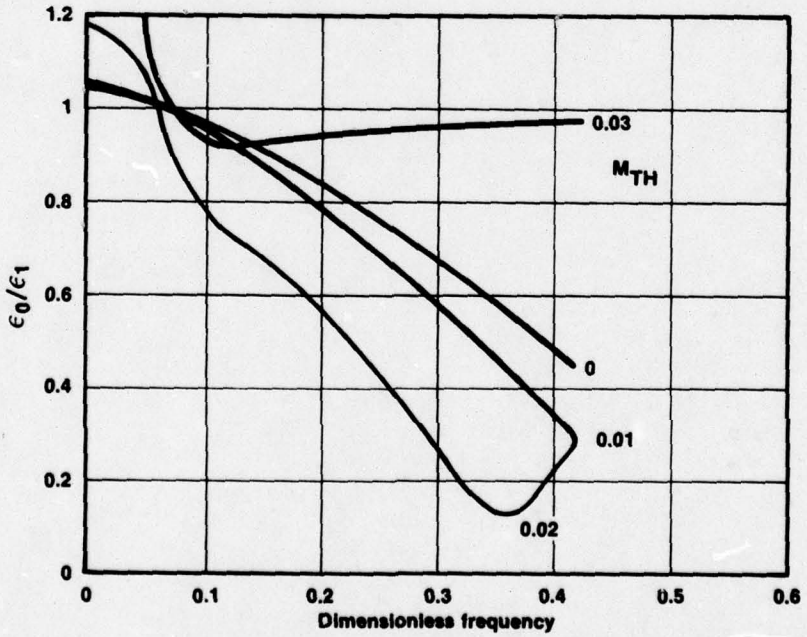

Figure 2-11. Ratio of Pressure Amplitudes (Input Response Based on ANB 3066)

V-10469

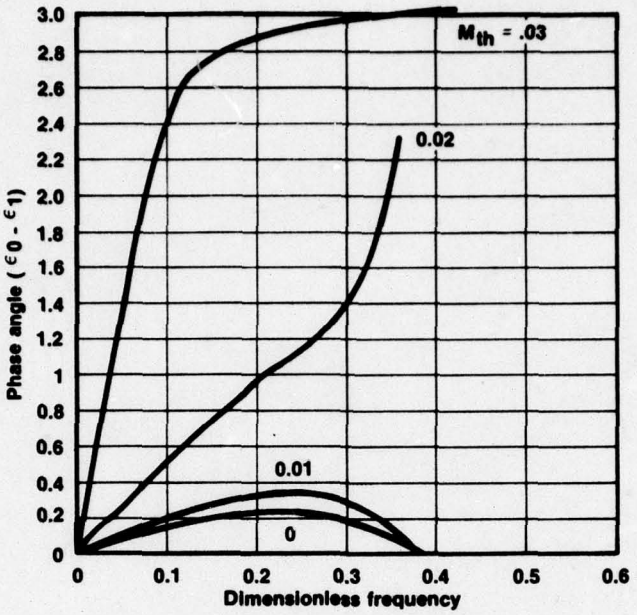

Figure 2-12. Phase of Pressure at Z = 0 to Pressure at Z = 1 (Input Responses Based on ANB 3066)

V-10470

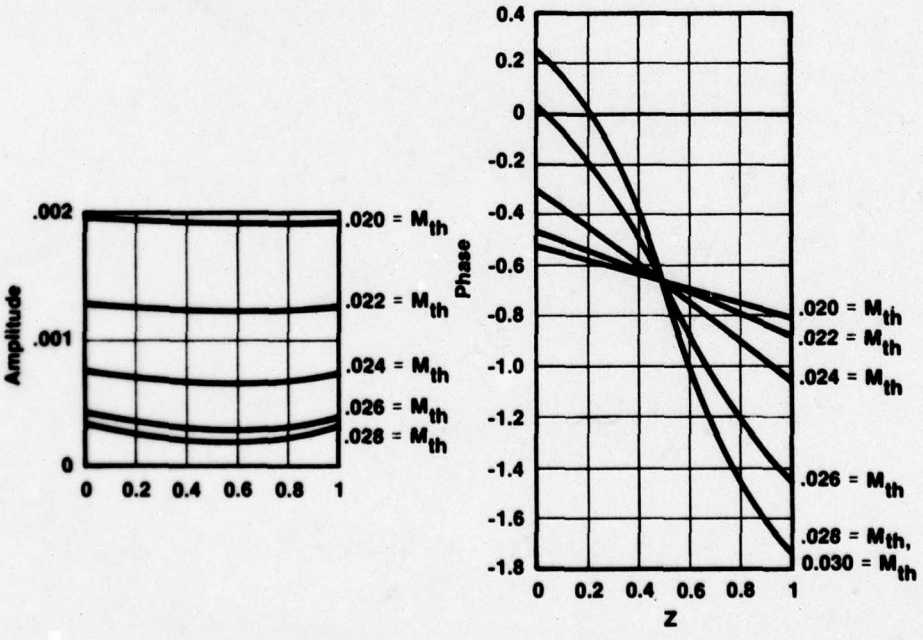

Figure 2-13. Effect of M_{th} on Phase of ϵ vs Z

V-10471

Additional studies are being conducted to examine the effects of amplitude dependent velocity coupling in greater detail. The objective is to derive a method for obtaining both the velocity response function and the threshold velocity from test data. These studies are in progress but have not progressed sufficiently to warrant a discussion of the results.

2.2 EXPERIMENTAL STUDIES

2.2.1 Apparatus Description

A dual rotating valve apparatus was designed and constructed under this program. The basic apparatus layout is shown schematically in figure 2-14. This arrangement provides the flexibility required to study both velocity coupled and pressure coupled configurations simply by changing the arrangement of holes in the graphite rotor sleeve.

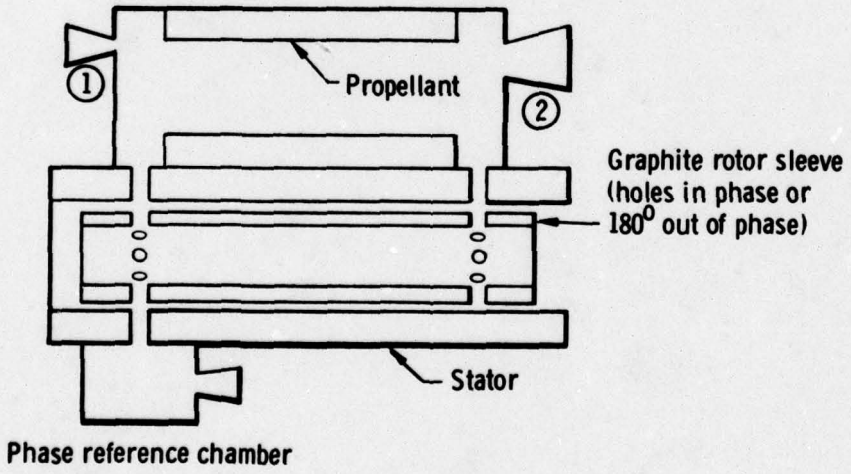

Figure 2-14. Apparatus Layout

08890

Figure 2-15 shows the essential components in exploded view. The rotor with a graphite sleeve is shown together with four graphite slots in their relative positions. The two slots on the upper left vent to the auxiliary chambers; those on the lower right vent to each end of the combustion chamber. A motor case loaded with propellant is also shown.

Figure 2-16 shows a photograph of the apparatus with a propellant grain being inserted into the combustion chamber. Figure 2-17 shows the steady-state nozzle and igniter wire inserted in preparation for a combustion test.

Kistler pressure transducers are located at each end of the grain to monitor the oscillating component of pressure. In addition, a Taber transducer monitors the average chamber pressure. The valve at each end of the chamber also has an auxiliary chamber that serves as a phase reference for

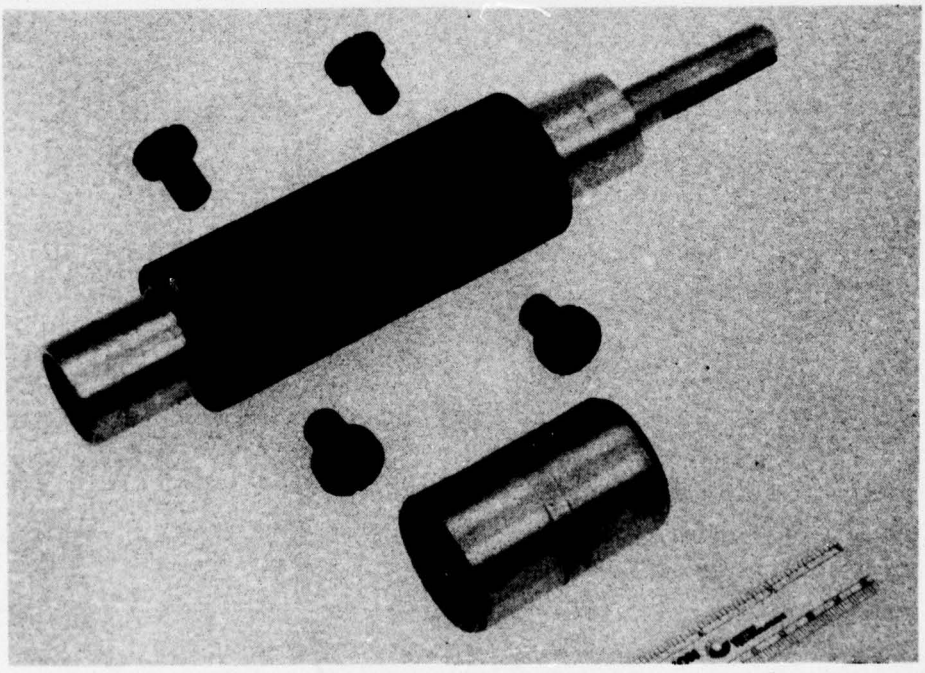

Figure 2-15. Dual Rotating Valve Components

10900-11

12940

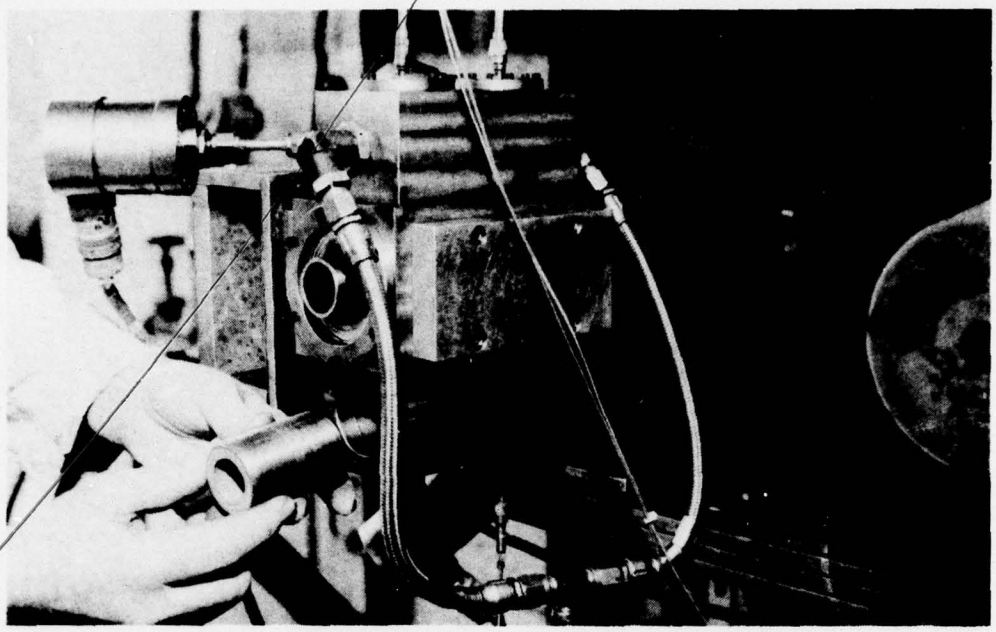

Figure 2-16. Propellant Grain and Valve Assembly

10900-5 12937

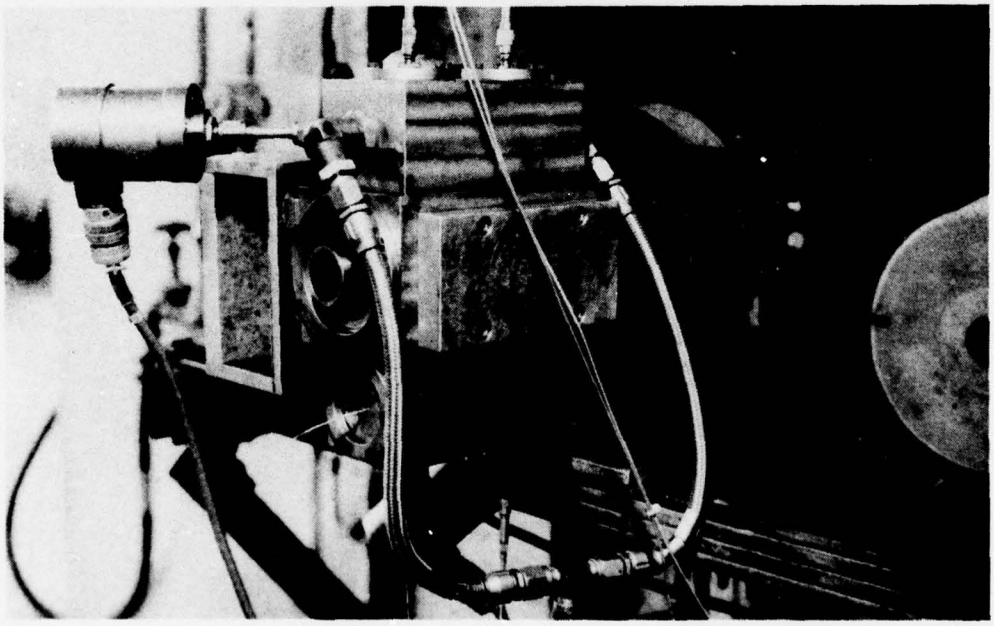

Figure 2-17. Assembled Rotating Valve Apparatus

10900-4 12938

each valve. Each is equipped with a Kistler and Taber transducer to monitor the oscillating pressure and the average chamber pressure. All the transducer outputs are recorded with an FM tape recorder and played back through appropriate filters and phase meters as described in references 6 and 7.

2.2.2 Cold Flow Tests

Cold flow tests were conducted as the first step in experimentally evaluating this apparatus. In these studies, nitrogen was injected into the combustion chamber and the two auxiliary chambers through individual sonic chokes. The discharge coefficients of all three exhaust nozzles were evaluated by calibration against a standard venturi flow meter. Under these conditions the response functions are zero, and the analysis described in the previous section can be used to predict the ballistics of all three chambers.

The first series of tests was conducted using a rotor sleeve, where the two rows of holes were in phase, i.e., the pressure coupled configuration. Figure 2-18 shows the excellent agreement between the predicted and observed amplitude in all three chambers. These tests were conducted at frequencies between 100 and 250 Hz using the clockwise-counterclockwise method of reference 6.

The corresponding phase comparison, shown in figure 2-19, used the oscillating pressure in the combustion chamber as a reference. Again, excellent agreement was obtained between the predicted and observed phase differences. These results are important because they demonstrate that the operation of the apparatus is basically sound.

These initial tests were conducted using only one Kistler pressure transducer in the combustion chamber. However, the analytical studies described in paragraph 2.1.3 showed that pressure measurements at each end of the burner are required. In addition, studies at AFRPL showed that replacing the graphite with 90% Ta 10% W increased the service life of the slots significantly. Both these changes were made and a second series of cold flow tests was conducted.

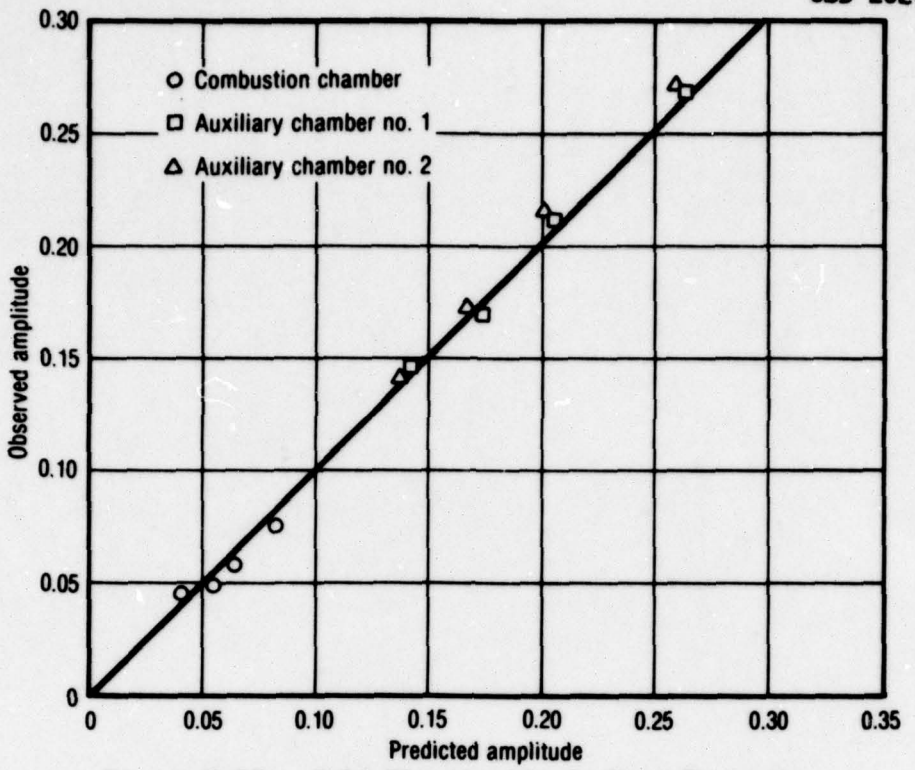

Figure 2-18. Cold Flow Amplitude Data Pressure Coupled Dual Valve Configuration

12941

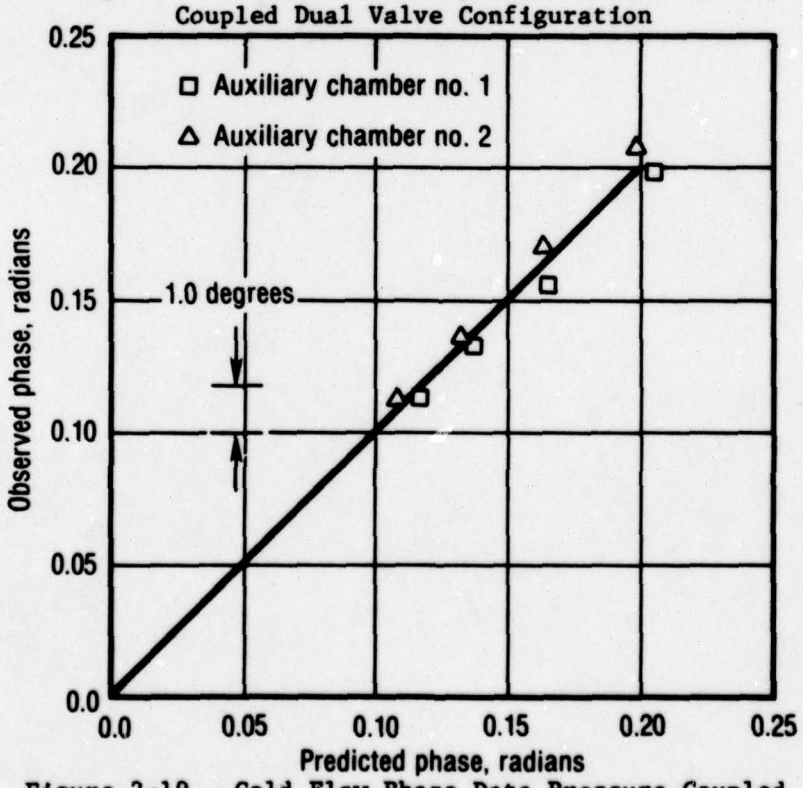

Figure 2-19. Cold Flow Phase Data Pressure Coupled Dual Valve Configuration (Combustion Chamber as Reference)

12942

The results from this second series of tests are shown in figures 2-20 through 2-23. They show excellent agreement between the predicted and measured amplitudes and phase angles. They also form an excellent basis for compensating for the effect of rotational direction on phase angle as described in reference 6.

2.2.3 Combustion Tests

Next, a series of combustion tests was conducted to evaluate the performance of the apparatus. The first tests were conducted with the standard rotating valve grains (2.75 in. long, by 1.0 in. diameter initial port with a 0.25 in. web) and a steady state nozzle at one end. Figure 2-24 shows the oscillating pressures at each end of the motor and the mean chamber pressure vs. time. The time delay in the rise of P_c and the appearance of oscillations resulted from delays in the release of the Kistler grounding circuit. Results are shown for various filter settings (Q) at the fundamental frequency and for the second harmonic content.

The most notable observations are the large amplitude modulations in the oscillating pressure. By imposing the condition that $\partial\varepsilon/\partial\tau = i\lambda\varepsilon$, the analysis does not permit evaluation of the modulations. To investigate their source, a series of tests was made using equal steady-state nozzles at each end of the motor. Under these conditions, the analysis predicts the amplitude of the oscillations should be extremely small. The test results shown in figure 2-25 show little change from the previous case.

Further study revealed that the frequency of the modulations is every twenty cycles, which equals the number of holes around the rotor. Careful review of the machining tolerances showed these rotors had minor variations in the spacing between holes. New rotors were machined to more exacting tolerances. Tests with these new rotors showed a substantial reduction in the magnitude of the modulations, as shown in figure 2-26. Hence the predominant source of the modulations appears to be in the machining tolerance of the graphite rotor sleeves.

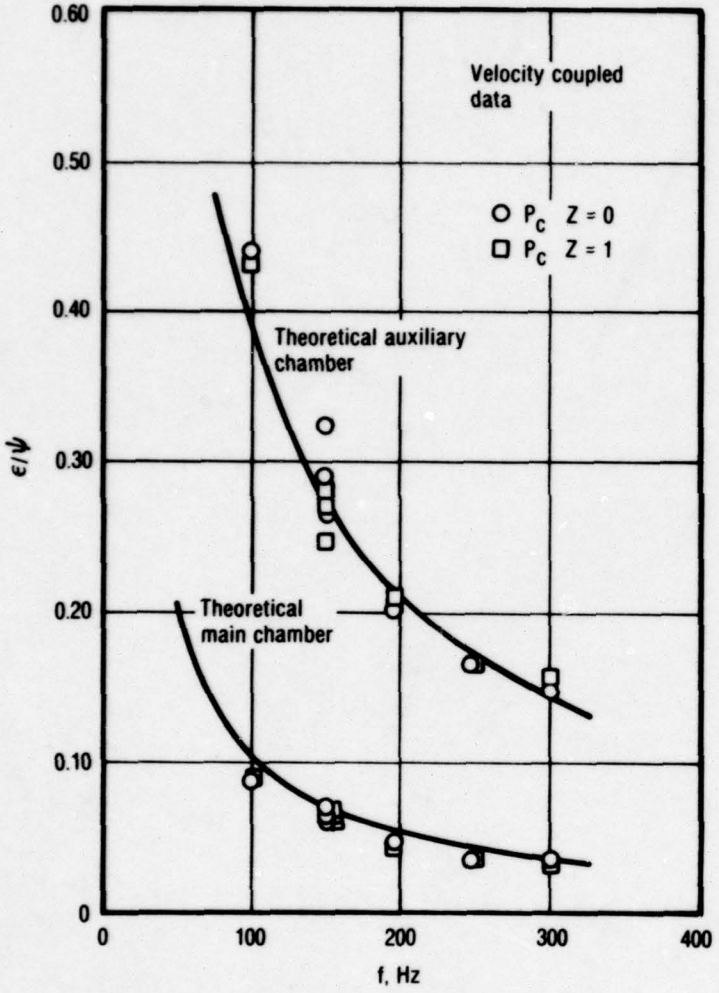

Figure 2-20. Cold Flow with Vent at Z = 0 Blocked (Tantalum Slots and Rotor Body Used)

15151

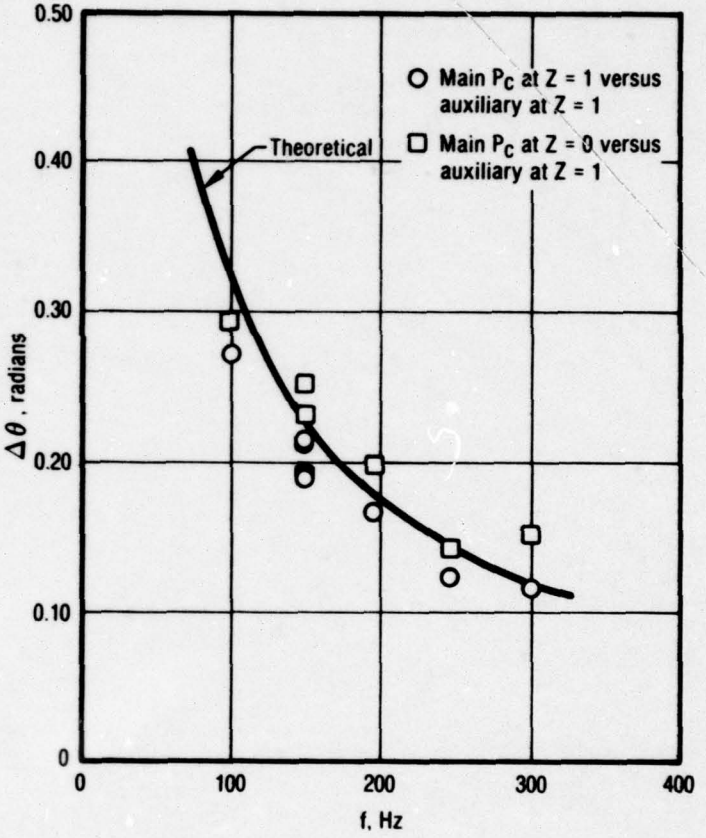

Figure 2-21. Cold Flow with Vent at Z = 0 Blocked (Tantalum Slots and Rotor Body Used)

15152

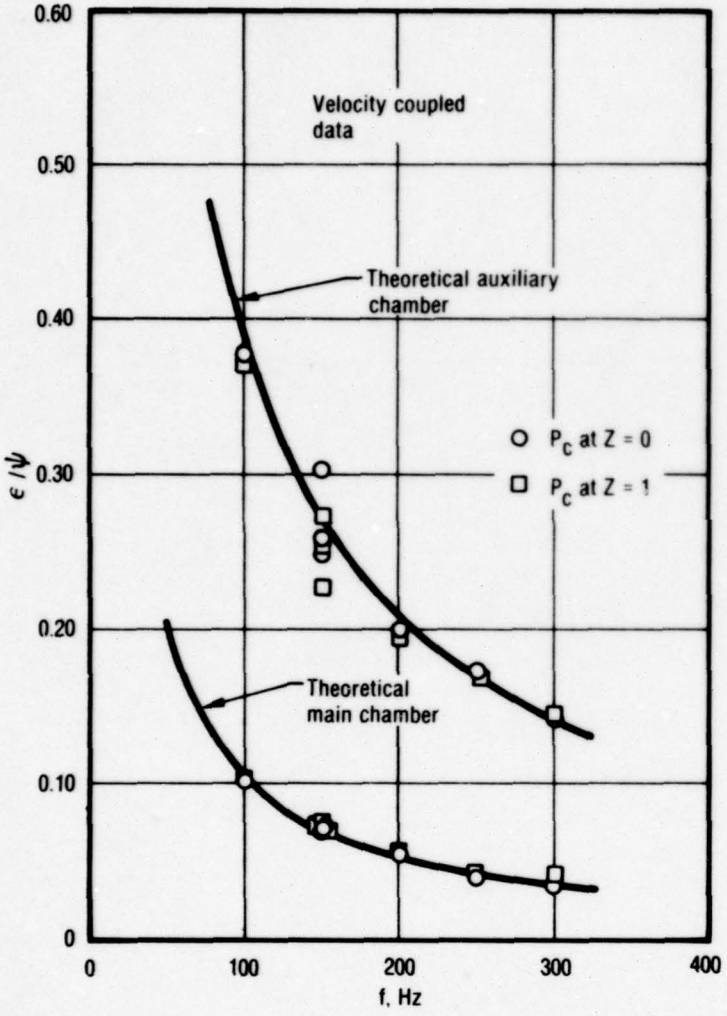

Figure 2-22. Cold Flow with Vent at Z = 1 Blocked (Tantalum Slots and Rotor Body Used)

15153

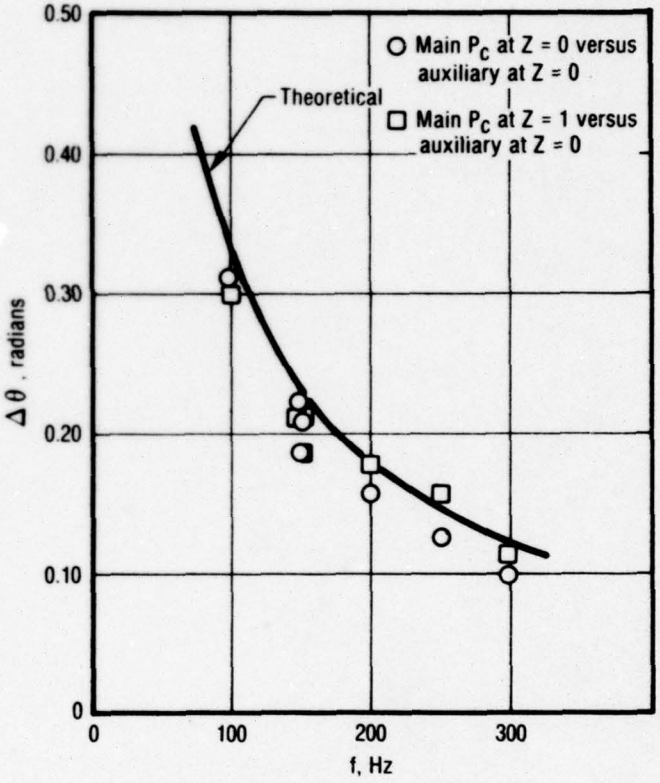

Figure 2-23. Cold Flow with Vent at Z = 1 Blocked (Tantalum Slots and Rotor Body Used)

15154

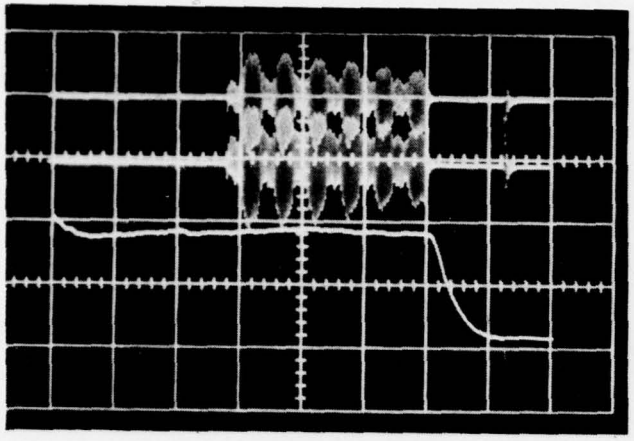

Fundamental frequency Q = 4

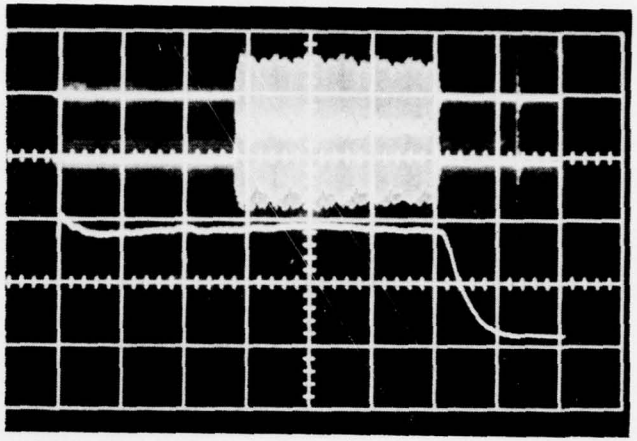

Second harmonic Q = 4

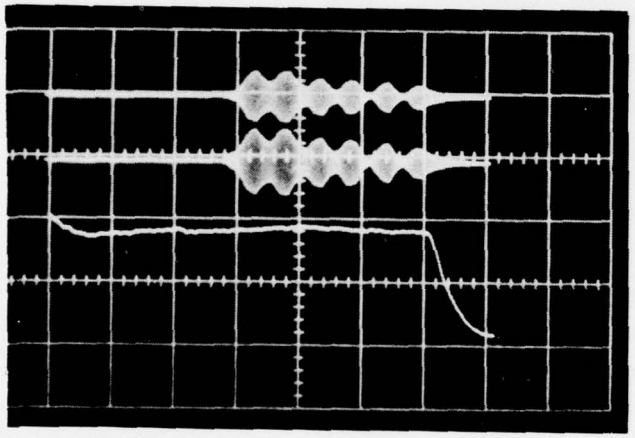

Fundamental frequency Q = 64

UTP-19,933

P_{osc} = 2 psi/cm

P_c = 500 psi/cm

Fundamental frequency = 300 Hz

Figure 2-24. Steady-State Nozzle at One End
(1-in.-Diameter Port)

V-09451

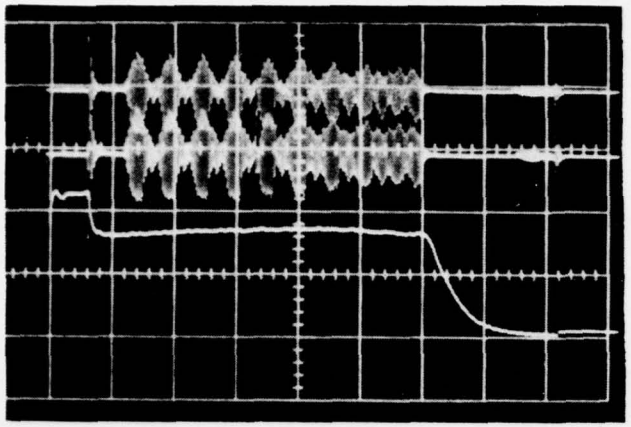

Fundamental frequency Q = 4

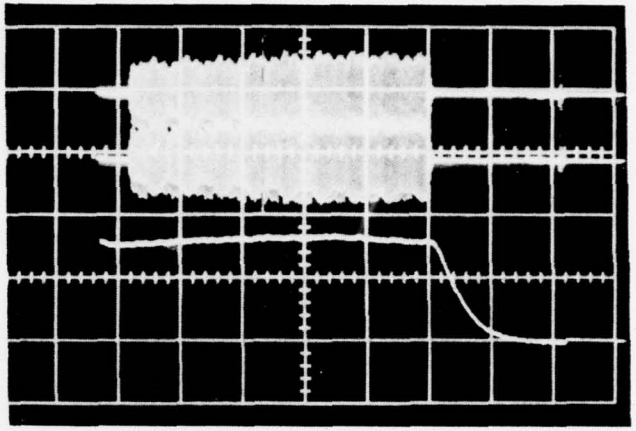

Second harmonic Q = 4

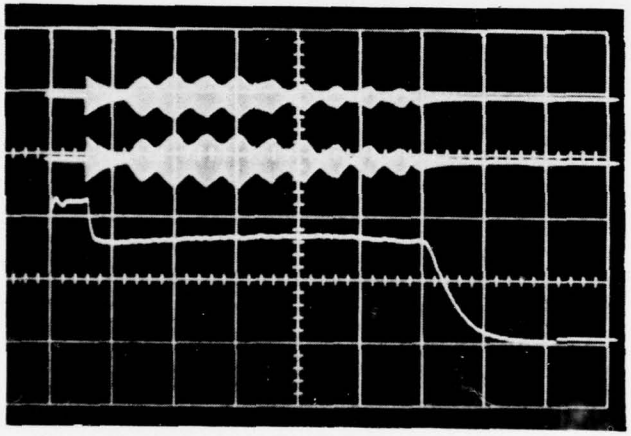

Fundamental frequency Q = 64

UTP-19,933

P_{osc} = 2.0 psi/cm

P_c = 500 psi/cm

Fundamental frequency = 300 Hz

Figure 2-25. Identical Steady State Nozzles at Each End (1-in.-Diameter Port)

V-09453

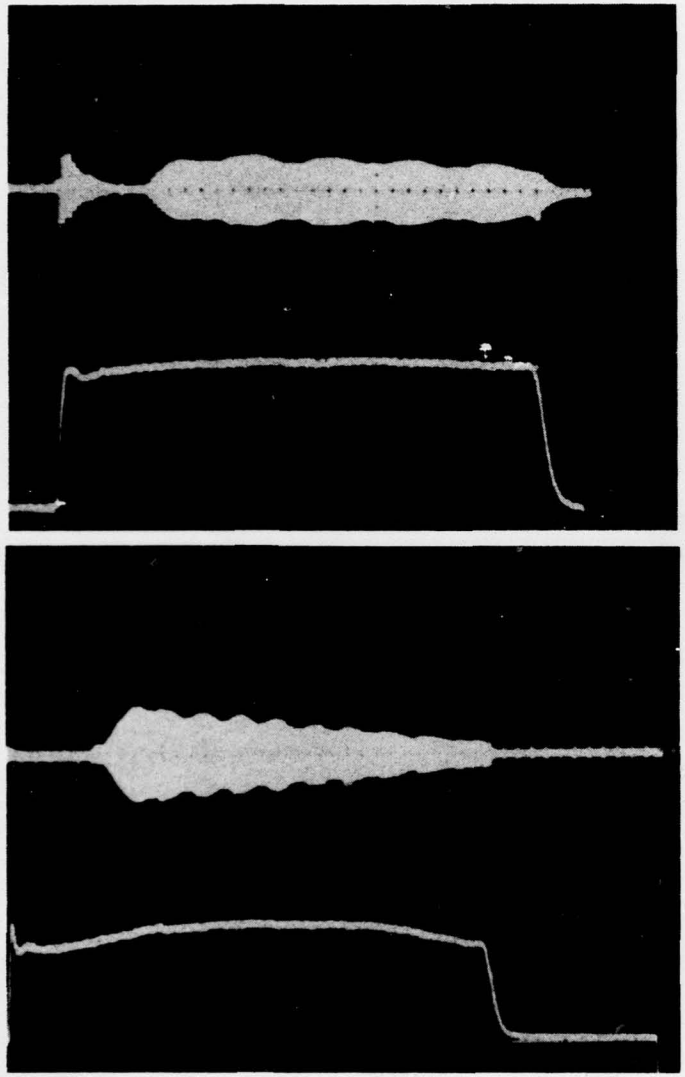

1 in. diameter port

P_{osc} = 20 psi/cm

P_c = 400 psi/cm

0.5 in. diameter port

P_{osc} = 20 psi/cm

P_c = 400 psi/cm

Figure 2-26. Data Using Improved Sleeve
(Test Frequency = 150 Hz)

V-10636

Tests were then conducted to evaluate the materials aspects of the apparatus performance. In particular these tests compared the graphite slot inserts with inserts made from 90% Ta, 10% W, as suggested by Hewes.[15] Both UTP-19,933, a nonaluminized formulation, and UTP-18,803A, a formulation containing 21% Al, were used. The results showed the metal inserts to be far superior to the graphite inserts. The metal insert at Z = 0 in figure 2-1 showed no significant deterioration. At Z = 1, however, the slot width in the metal insert appeared to increase slowly over several tests and then finally failed. The failure appeared to result from excessive erosion and melting. When graphite inserts were used, the Z = 1 location also showed slightly higher erosion rates than the Z = 0 location.

The reason for this apparent difference is not immediately clear. One possibility is a variation in the properties of the metal between the two inserts. However, a third metal slot insert was made from the same metal billet for the single rotating valve and has performed satisfactorily with highly metallized propellants. Another billet has been ordered and a new insert of the same material will be machined and tested to evaluate this possibility.

Another possibility is excessive heat transfer and erosion because of peculiar local flows. The slots have identical locations with respect to the grain. However, the steady state nozzle is located at Z = 1, so there are mean flow differences which could be responsible. However the failure occurred at the surface on the rotor, not at the inlet to the slot. Thus, further work is needed to study this potential problem.

It should be noted that Ta/W was also used in the rotor to support the graphite sleeves. This substitution for 303 stainless steel was found to be a definite improvement. No significant deterioration was observed and problems resulting from differential thermal expansion were eliminated.

Additional combustion tests were then conducted over a range of frequencies using UTP-19,942 and UTP-19,933. These propellants have been tested for pressure coupled response at CSD[16] and the limited data are shown summarized in figure 2-27. The imaginary part of the linear velocity response functions was derived from the data using equation (18) and is shown in figure 2-28.

Several observations can be made from these results. First, reasonable reproducibility was obtained. Second, there appears to be a significant difference between the two formulations tested. The only difference in these compositions is that UTP-19,942 contains 0.5% of the copper combustion modifier reported in reference 16. This additive did reduce the driving of high frequency combustion instabilities and it could be postulated that the effect is through modification of the gas phase combustion process. Thus, one could argue that perhaps the modifier could also alter the velocity response properties as well. Obviously, however, more data are required to substantiate this preliminary speculation.

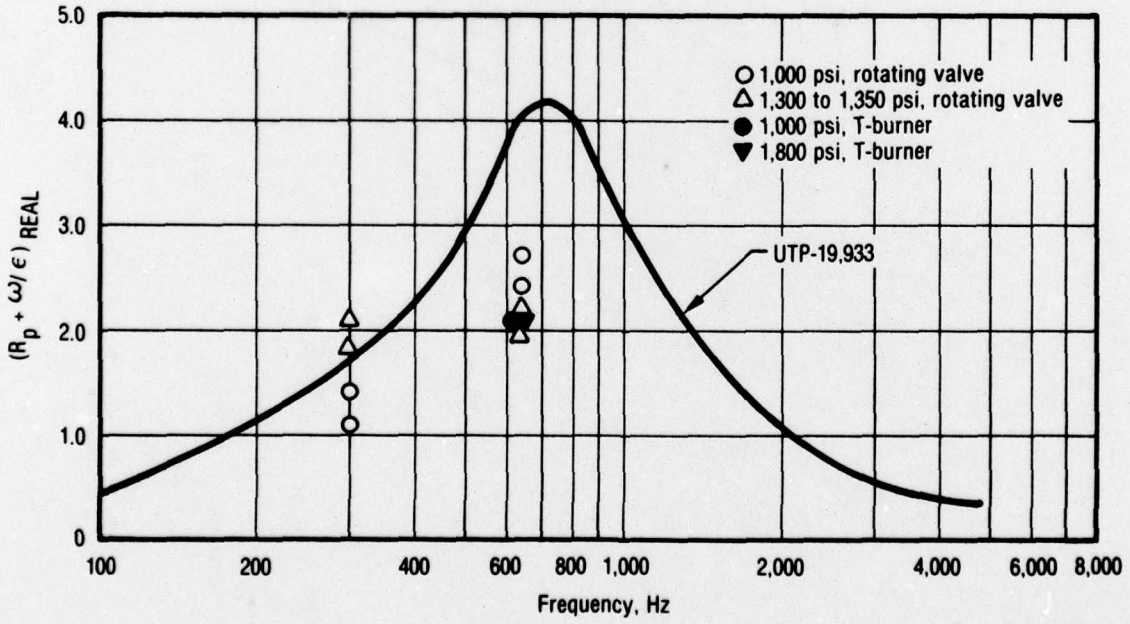

Figure 2-27. Combustion Response of UTP-19,942

13649

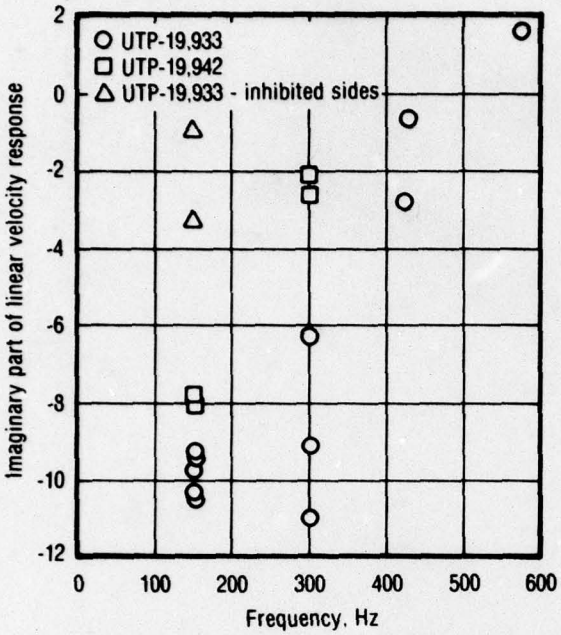

Figure 2-28. Linear Velocity Response
15155

Comparing the results with the hypotheses of Culick[8] and Price[13,14] for linear velocity response shows an inconsistency between the data and predictions. The hypotheses suggest the response is positive at lower frequencies and then becomes negative at higher frequencies. The data suggest the velocity response is negative at low frequencies and becomes positive at higher frequencies. More data are needed to determine if the response extrapolates to zero as the frequency approaches zero as suggested by Culick and Price.

Two additional tests were conducted to evaluate grain geometry changes. The analytical model assumes all the burning surface regresses radially and there are no end burning surfaces. The grains, however, do have end burning surfaces to provide a neutral pressure-time trace. Hence, initially in the burning there is a burning surface which is not subject to velocity oscillations parallel to the burning surface. To minimize this effect, the results shown in figure 2-28 were derived near the end of each test where the end burning area was smallest.

To explore this effect further, two tests were conducted using grains with inhibited end surfaces. The derived linear velocity response function obtained from these tests is shown in figure 2-28 as well. There appears to be a significant effect on the inhibitor. It should be noted that the pressure time traces from these tests deviated somewhat from the predicted curves and appeared as though the inhibitor was only partially effective. It is apparent, however, that more testing is required to resolve the mechanisms producing this effect.

Another possible framework for characterizing velocity response is the nonlinear model suggested by Price[13,14] and by Culick.[8] The nonlinearity of this model would produce a high harmonic content in the pressure wave. Hence, data analyses were conducted to investigate possible nonlinear effects. Amplitude spectra analysis from two tests, both conducted at 300 Hz using neutral burning grains, are shown in figures 2-29 and 2-30. These spectra were obtained using a Hewlett-Packard Model 3582A Spectrum Analyzer. The data shown in figure 2-29 were obtained using one steady-state nozzle while the data in figure 2-30 were obtained using identical steady-state nozzles at each end of the burner.

Several observations can be made. First, both figures show significant harmonic content. Analysis of the driver wave form[5] shows no driving of the even harmonics by the valve and only minimal (-25 dB) driving of the third harmonic. Thus, the energy at the even harmonics is produced by the fluid mechanics of the burner and not by the rotating valve driver. Furthermore, the energy at the odd harmonics is substantially larger than would be expected from the linear model. Hence, in this instance, linear velocity coupling could not produce this frequency spectrum.

Preliminary studies were then made to determine if the nonlinear velocity coupling model could account for the observed harmonic content. The model calculates the harmonic content of the burning rate oscillation for a given threshold velocity and amplitude of the velocity oscillation. The combustor was assumed to transform these oscillations by a "bulk mode" response. Initial calculations indicate the predicted harmonic content is significantly less than the observed content. However, additional parametric studies are needed over a wider range of conditions and formulations to reach a firm conclusion.

Another source of the high harmonic content could result from nonlinear flow effects. For example, the linearization of the momentum equation assumes the mean flow velocity is much larger than the Mach number of the oscillating flow at every axial position. Since there is mean flow from both ends of the

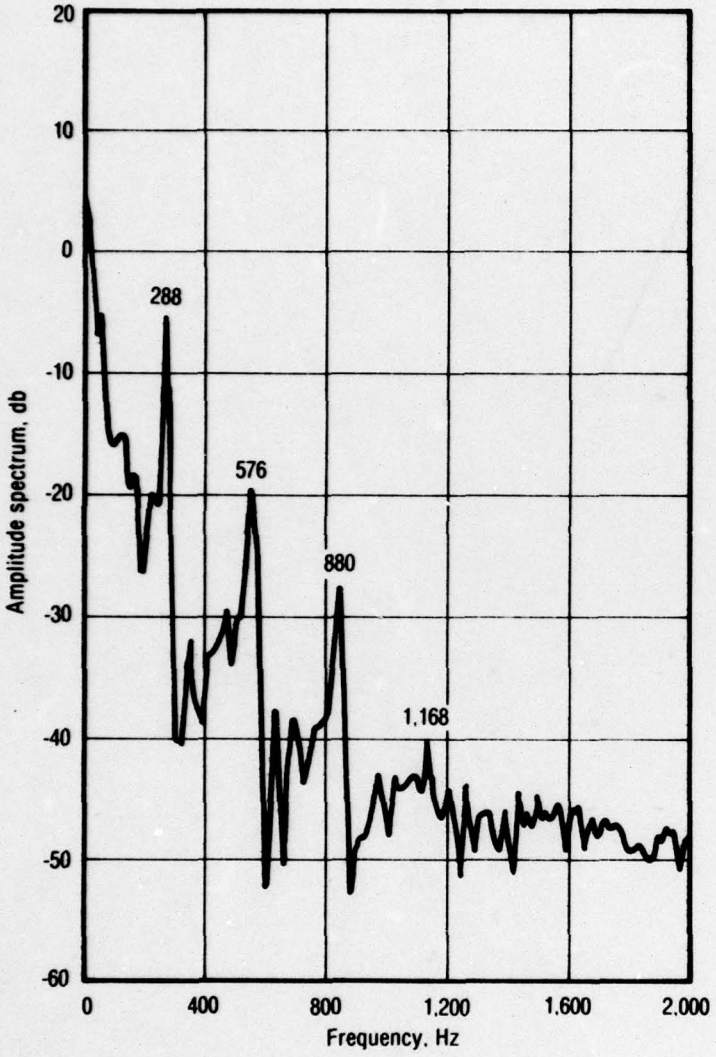

Figure 2-29. Power Spectra Analysis

15156

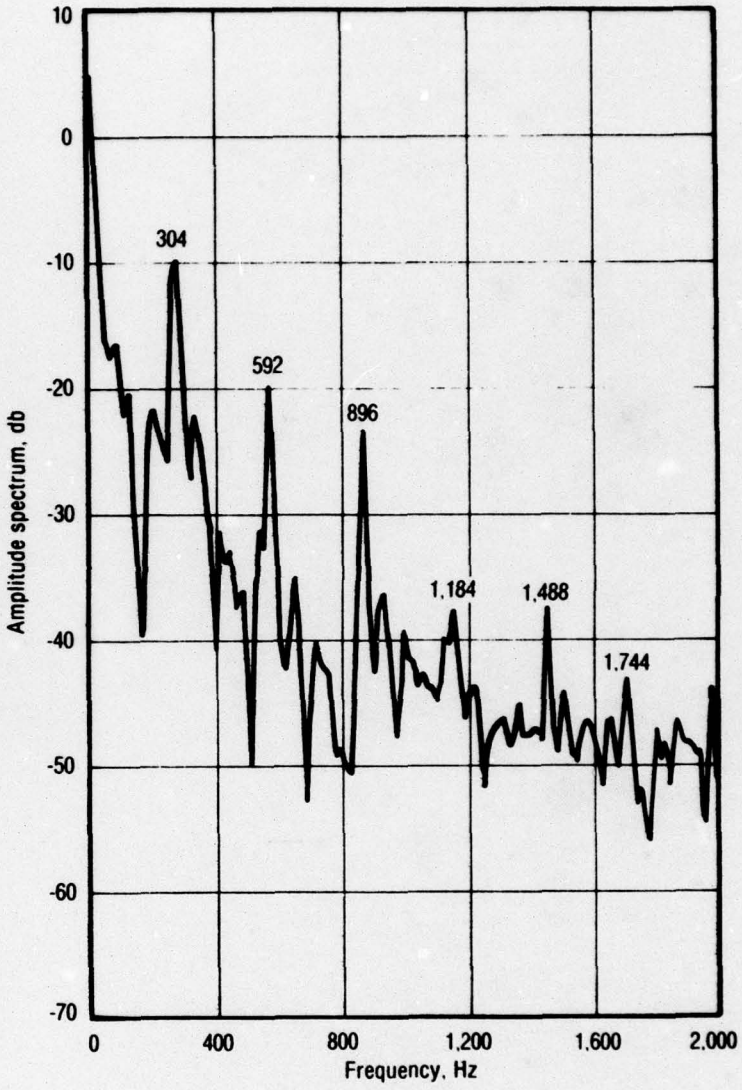

Figure 2-30. Power Spectra Analysis

15157

burner, the mean flow Mach number is zero at some point along the axis, more precisely at ($Z = \overline{\chi}_1$). The oscillating flow Mach number is essentially constant along the axis. Hence, the assumption breaks down in the region where $\overline{M} = 0$. Including this extra term introduces a nonlinearity which ultimately could contribute to the harmonic content. The counter argument to this point is that this flow nonlinearity enters through the momentum equation. At low frequencies, momentum effects are relatively unimportant; hence, the nonlinearity should not be important. At this date, this point remains unresolved.

3.0 CONCLUSIONS

A one-dimensional analysis of the dual rotating valve has been developed. This model is based on linear fluid dynamics and includes both a linear and an amplitude dependent velocity coupling model. The effects of pressure coupling, flow turning, and particle damping are also included. Parametric and analytical studies show the equations reduce to the proper bulk mode behavior at low frequencies. The analysis also predicts the proper damping of the natural acoustic modes of the motor.

Cold flow studies confirm the predicted behavior for the pressure coupled configuration. In the velocity coupled configuration, control of the phase angle between the two valves was found to be extremely important. Methods and specifications were developed for achieving the necessry accuracy.

Combustion tests have been conducted using both nonaluminized and aluminized propellants. With the possible exception of materials problems in one area, satisfactory apparatus performance was demonstrated. Velocity response functions were found to increase from -10 at 150 Hz to 1.6 at 600 Hz for the linear model. Differences in response were observed with a change in propellant composition.

Frequency spectra analysis of the pressure oscillations shows significant harmonic content which suggests contributions form nonlinear or amplitude dependent processes. Attempts to explain this harmonic content with the amplitude depdendent velocity coupling model have not been successful to date.

Thus, the combustion data obtained to date requires further study and supporting evidence before a satisfactory evaluation of the two velocity coupling models can be developed.

4.0 PUBLICATIONS ON THIS PROJECT

1. Brown, R. S., Willoughby, P. G., and Kelly, V. L., "Rotating Valve for Velocity Coupling Combustion Response Studies," AIAA Paper 77-975 presented at AIAA 13th Propulsion Conference, Orlando, FL, 1977.

2. Brown, R. S., Waugh, R. C., and Kelly, V. L., "Rotating Valve for Velocity Coupling Combustion Response Studies," paper presented at 15th JANNAF Combustion Conference, Newport RI, September 11-15, 1978.

3. Brown, R. S. and Waugh, R. C., "Pressure and Velocity Response Function Measurements by the Rotating Valve Method." paper to be presented at AGARD 53rd PEP Symposium, Oslo, Norway, April 2-5, 1979.

REFERENCES

1. Brown, R. S., Willoughby, P. G., and Kelly, V. L., "Rotating Valve for Velocity Coupled Combustion Response Studies," AIAA paper 77-975 presented at AIAA 13th Propulsion Conference, Orlando, FL, July 1977.

2. Culick, F. E. C., "The Stability of One Dimensional Motions in a Rocket Motor," Combustion Science and Technology, Volume 7, pp. 165-175, 1973.

3. Murphy, G. M., Ordinary Differential Equations and Their Solutions, Van Nostrand Reinhold Company, New York, pp. 323, 1960.

4. Abramowitz, M. and Stegun, I. A., "Handbook of Mathematical Functions with Formulas, Graphs, and Mathematical Tables," National Bureau of Standards Applied Mathematics Series No. 55, 1964.

5. Brown, R. S., Erickson, J. E., and Babcock, W. R., "Combustion Instability Study of Solid Propellants," AIAA Journal, Volume 12, pp. 1502-1510, 1974.

6. Brown, R. S., "Development and Evaluation of Rotating Valve Combustion Response Test Techniques", AFRPL-TR-75-72, October 1976.

7. Brown, R. S., and Muzzy, R. J., "Linear and Nonlinear Pressure Coupled Combustion Instability of Solid Propellants," AIAA Journal, Volume 8, pp. 492-1,500, 1970.

8. Culick, R. E. C., "Stability of Longitudinal Oscillations with Pressure and Velocity Coupling in a Solid Propellant Rocket," Combustion Science and Technology, Volume 2, pp. 179-201, 1970.

9. Langelle, G., "A Model Describing the Velocity Response of Composite Propellants," AIAA Journal, Volume 13, pp. 315-322, 1975.

10. Beckstead, M. W. and Butcher, A. G., "The Velocity Coupled T-Burner," AIAA Preprint No. 74-200 presented at 13th Aerospace Sciences Meeting, Washington, DC, 1974.

11. Micheli, P. L., "Investigation of Velocity Coupled Combustion Instability," AFRPL Report No. TR-76-100, Aerojet Solid Propulsion Company, 1977.

12. Lovine, R. L., Dudley, D. P., and Waugh, R. C., "Standardized Stability Prediction Method for Solid Rocket Motors," AFRPL-TR-76-32, Aerojet Solid Propulsion Company, May 1976.

13. Price, E. W. and Dehority, G. L., "Velocity Coupled Axial Mode Combustion Instability in Solid Propellant Rocket Motors," ICRPG/AIAA 2nd Solid Propulsion Conference (June 1967) pp. 213-227.

14. Dehority, G. L., and Price, E. W., "Axial Mode, Intermediate Frequency Combustion Instability in Solid Propellant Rockets," Naval Weapons Center Report NWC-TP-5654, October 1974.

15. Hewes, J. C., private communication 1977.

16. Rudy, T. P., Bain, L. S., and Newnan, B. D., "Chemical Control of Propellant Combustion", AFRPL-TP-78-15, Chemical Systems Division, April 1978.

UNCLASSIFIED

SECURITY CLASSIFICATION OF THIS PAGE (When Data Entered)

(18) (19) REPORT DOCUMENTATION PAGE

READ INSTRUCTIONS BEFORE COMPLETING FORM

1. REPORT NUMBER: AFOSR-TR-79-0247	2. GOVT ACCESSION NO. (9) Annual technical rept.
4. TITLE (and Subtitle): (6) Rotating Valve for Velocity Coupled Combustion Response Measurements.	5. TYPE OF REPORT & PERIOD COVERED: INTERIM 1 Jan 78 to 9 Jan 79
	6. PERFORMING ORG. REPORT NUMBER: (14) CSD-2624-ISR-2
7. AUTHOR(s): (10) R. S. Brown and R. C. Waugh	8. CONTRACT OR GRANT NUMBER(s): (15) F49620-77-C-0048
9. PERFORMING ORGANIZATION NAME AND ADDRESS: Chemical Systems Division, United Technologies, P. O. Box 358, Sunnyvale, CA 94088	10. PROGRAM ELEMENT, PROJECT, TASK AREA & WORK UNIT NUMBERS: (16) 2308A1, 61102F (17) A1
11. CONTROLLING OFFICE NAME AND ADDRESS: AIR FORCE OFFICE OF SCIENTIFIC RESEARCH/NA, BLDG 401, BOLLING AIR FORCE BASE, D C 20332	(11) 12. REPORT DATE: 24 February 1979; 13. NUMBER OF PAGES: 50
14. MONITORING AGENCY NAME & ADDRESS (if different from Controlling Office): (12) 53p.	15. SECURITY CLASS. (of this report): Unclassified; 15a. DECLASSIFICATION/DOWNGRADING SCHEDULE

16. DISTRIBUTION STATEMENT (of this Report)

Approved for public release; distribution unlimited.

17. DISTRIBUTION STATEMENT (of the abstract entered in Block 20, if different from Report)

18. SUPPLEMENTARY NOTES

19. KEY WORDS (Continue on reverse side if necessary and identify by block number)

Rotating Valve
Combustion Stability
Solid Propellant Combustion

20. ABSTRACT (Continue on reverse side if necessary and identify by block number)

Coupling between the combustion process and the acoustics of the combustion chamber are important factors determining combustion stability of a solid propellant rocket. This coupling results from the response of the combustion process to both the local acoustic pressure and the local acoustic velocity. Because of the complexity of both processes, they cannot be totally characterized analytically; therefore, laboratory test data are needed in making analytical combustion stability predictions. (Continued)

DD FORM 1 JAN 73 1473 EDITION OF 1 NOV 65 IS OBSOLETE

391927

UNCLASSIFIED

SECURITY CLASSIFICATION OF THIS PAGE (When Data Entered)

20. ABSTRACT (Continued)

Under AFOSR contract No. F49620-77-C-0048, CSD is investigating the dual valve approach for measuring velocity coupled characteristics in greater detail. Analytical studies accomplished under this contract have developed a mathematical analysis of the transient ballistics. The solution of the transient mass, momentum, and energy equations incorporates both linear and nonlinear velocity coupling, as well as pressure coupling, particle damping, flow turning, and nozzle losses in the analysis. The analysis shows that velocity coupling dominates the system response when the two valves operate 180° out of phase.

The analytical solutions agree with known solutions for low frequency bulk mode conditions and for the frequency response characteristics at acoustic resonance. Studies have been conducted to explore its limitations and to estimate the effects of experimental uncertainties. Approximate solutions have been developed which permit the direct derivation of velocity response functions from experimental data assuming linear velocity coupling. Parametric studies were also made using the nonlinear velocity coupling model. The results show the interaction of mean velocity magnitude, threshold velocity, and amplitude of the velocity oscillation on the predicted pressure oscillations. Some progress has been made towards developing an approximate solution for data reduction purposes but more development is needed to develop a useful method.

Concurrently, an experimetal apparatus was constructed, and its performance under controlled cold flow conditions was compared with predictions. Agreement between predicted and experiment behavior was demonstrated under pressure-coupled conditions. In the velocity-coupled mode, the cold flow tests showed control of the phase angle between the two valves is important to ensure proper performance of the apparatus. Apparatus improvements were made to achieve this control.

Combustion tests were ~~then~~ conducted using two nonaluminized propellants. Analysis of the data, using the linear velocity response model, indicates the imaginary part of the response increases from approximately -10 at 150 Hz to approximately 1.6 at 570 Hz. Amplitude spectrum analyses of the pressure traces show significant harmonic content. Since the area wave form contains very low harmonic content, this suggests the nonlinear velocity coupling may provide a more realistic framework for data interpretation. Combustion tests were also conducted with a formulation containing 21% aluminum. With the exception of one slot insert, the apparatus operated satisfactorily. The failure of one slot insert after several tests appears to be the result of faulty materials.